HAL
open science

Kinematics of fluid particles on the sea surface. Hamiltonian theory

Francesco Fedele, Cristel Chandre, Mohammad Farazmand

To cite this version:

Francesco Fedele, Cristel Chandre, Mohammad Farazmand. Kinematics of fluid particles on the sea surface. Hamiltonian theory. Journal of Fluid Mechanics, 2016, 801, pp.260. 10.1017/jfm.2016.453 . hal-01207149

HAL Id: hal-01207149

https://hal.science/hal-01207149v1

Submitted on 30 Sep 2015

HAL is a multi-disciplinary open access archive for the deposit and dissemination of scientific research documents, whether they are published or not. The documents may come from teaching and research institutions in France or abroad, or from public or private research centers.

L'archive ouverte pluridisciplinaire **HAL**, est destinée au dépôt et à la diffusion de documents scientifiques de niveau recherche, publiés ou non, émanant des établissements d'enseignement et de recherche français ou étrangers, des laboratoires publics ou privés.

arXiv:1509.08526v1 [physics.ao-ph] 28 Sep 2015

Kinematics of fluid particles on the sea surface. Part 1. Hamiltonian theory

F. Fedele[1,2]†, C. Chandre[3] and M. Farazmand[4]

[1]School of Civil and Environmental Engineering, Georgia Institute of Technology, Atlanta, GA 30322, USA

[2]School of Electrical and Computer Engineering, Georgia Institute of Technology, Atlanta, GA 30322, USA

[3]Centre de Physique Théorique - CNRS/Aix-Marseille University, 13009 Marseille, France

[4] Center for Nonlinear Sciences, School of Physics, Georgia Institute of Technology, Atlanta, GA 30332, USA

(Received September 30, 2015)

We derive the John-Sclavounos equations describing the motion of a fluid particle on the sea surface from first principles using Lagrangian and Hamiltonian formalisms applied to the motion of a frictionless particle constrained on an unsteady surface. The main result is that vorticity generated on a stress-free surface vanishes at a wave crest when the horizontal particle velocity equals the crest propagation speed, which is the kinematic criterion for wave breaking. If this holds for the largest crest, then the symplectic two-form associated with the Hamiltonian dynamics reduces instantaneously to that associated with the motion of a particle in free flight, as if the surface did not exist. Further, exploiting the conservation of the Hamiltonian function for steady surfaces and traveling waves we show that particle velocities remain bounded at all times, ruling out the possibility of the finite-time blowup of solutions.

Key words: Lagrangian; kinematics; fluid particles; Hamiltonian; wave breaking; symplectic.

1. Introduction

The horizontal motion of fluid particles on a zero-stress interface that separates water from air obeys a set of nonlinear ordinary differential equations, which only depend on the surface and its space-time gradient and curvature. John (1953) derived the equations of motion for such particles on the free surface of two-dimensional (2-D) gravity waves, and Sclavounos (2005) generalized them to the three dimensional (3-D) waves. In particular, given a Cartesian reference system (x, y, z), where z is along the vertical direction, he exploited the property that the zero-stress free surface $z = \zeta(x, y, t)$ is an iso-pressure surface, and thus the hydrodynamic pressure gradient $\nabla_3 p$ is collinear with the outward normal $\mathbf{n} \sim \nabla_3(z - \zeta)$ to the surface, where $\nabla_3 = (\partial_x, \partial_y, \partial_z)$. This implies that on the free surface

$$\nabla_3(z - \zeta) \times \nabla_3 p = \mathbf{0}, \qquad z = \zeta. \tag{1.1}$$

† Email address for correspondence: fedele@gatech.edu

From Euler's equations, the acceleration of a fluid particle in a 3-D flow satisfies

$$\frac{d^2\mathbf{r}}{dt^2} = -\frac{1}{\rho}\nabla_3 p + \mathbf{f},$$

where $\mathbf{r} = (x(t), y(t), z(t))$ is the instantaneous vector position of the fluid particle and $\mathbf{f} = (0, 0, -\mathrm{g})$ is the force due to gravitational acceleration g. Then, Eq. (1.1) can be written as

$$(-\partial_x\zeta\mathbf{i} - \partial_y\zeta\mathbf{j} + \mathbf{k}) \times \left(-\frac{d^2\mathbf{r}}{dt^2} + \mathbf{f}\right) = 0, \tag{1.2}$$

where $(\mathbf{i}, \mathbf{j}, \mathbf{k})$ are unit vectors along the x, y and z directions, respectively. The z component of the cross product (1.2) is redundant as it is a linear combination of the x and y components. These yield the coupled equations

$$\begin{aligned} \partial_y\zeta\left(\tfrac{d^2z}{dt^2} + \mathrm{g}\right) + \tfrac{d^2y}{dt^2} = 0, \\ \partial_x\zeta\left(\tfrac{d^2z}{dt^2} + \mathrm{g}\right) + \tfrac{d^2x}{dt^2} = 0. \end{aligned} \tag{1.3}$$

Since the fluid particle is constrained on the free surface ζ, its vertical velocity $\dot{z} = \frac{dz}{dt}$ and acceleration $\ddot{z} = \frac{d^2z}{dt^2}$ depend on the horizontal motion $\mathbf{x} = (x(t), y(t))$. In particular, $\ddot{z}$ follows from differentiating $z(t) = \zeta(x(t), y(t), t)$ with respect to time. Substituting the resulting $\ddot{z}$ in Eq. (1.3) yields the John-Sclavounos (JS) equations for the evolution of the horizontal fluid particle trajectories driven by the free-surface elevation and its Eulerian temporal and spatial derivatives.

To the best of authors' knowledge, the properties of the JS equations have not been investigated in great details, if not at all. In this work, we derive and study these equations using first principles in order to gain mathematical and physical insights into the dynamics of ocean waves and the inception of wave breaking.

2. Main findings

We demonstrate that the JS equations are more general than initially thought as they can be derived from first principles using Lagrangian and Hamiltonian formalisms. In particular, the Lagrangian formalism highlights a fundamental property of the JS equations. On the one hand, these are originally derived from the dynamical condition that the zero-stress free surface $z = \zeta$ is an iso-pressure surface (Sclavounos 2005). On the other hand, we have derived the same equations from an action principle describing the constrained motion of a frictionless particle on an unsteady surface and subject to gravity. The unsteady surface is arbitrary and can originate from many physical processes. In this regard, if we are interested in the fluid particle kinematics on the free surface of gravity water waves, then one needs to know the irrotational flow field that generates a zero-stress free surface separating water from air. Indeed, only if the initial particle velocity is set as that induced by the irrotational flow do the JS equations describe the kinematics of fluid particles.

For the shallow-water equations, the relation between the symplectic structure and physical vorticity is recently explored by Bridges *et al.* (2005). Here, similarly, our analysis of the Hamiltonian structure of the JS equations reveals that the associated symplectic one-form is the physical fluid circulation and certain terms of the associated two-form relate to the vorticity created on the zero-stress free surface. Furthermore, we find that vorticity created at a zero-stress free surface vanishes at a wave crest when the horizontal

particle velocity equals the propagation speed of the crest. This is the kinematic criterion for wave breaking (Perlin *et al.* 2013; Shemer & Liberzon 2014; Shemer & Ee 2015). If this holds for the largest crest, then the symplectic two-form instantaneously reduces to that associated with the motion of a particle in free flight, as if the free surface and vorticity did not exist at all.

In realistic oceanic fields the large crest eventually breaks and energy of fluid particles is dissipated to turbulence as a clear manifestation of time irreversibility. We speculate that this behavior appears analogous to a flight–crash event in fluid turbulence, where a particle flies with a large velocity before suddenly losing energy (Xu *et al.* 2014). Clearly, the Hamiltonian particle dynamics is time-reversible and the instantenous vanishing of vorticity at large crests may reveals the inviscid mechanism of breaking inception before turbulent dissipative effects take place. This then necessitates a further study of the dynamics and energetics of the wave field that generates the free surface to verify if the kinematic breaking criterion is valid.

In this regard, recent studies indicate that the inception of breaking of the largest crest of unsteady wave groups initiates when the particle velocity u_x exceeds about 0.84 times the crest velocity V_c (Barthelemy *et al.* 2015*b*; Saket *et al.* 2015). In particular, none of the non-breaking or recurrent groups reach the threshold $B_x = u_x/V_c = 0.84$, while all marginal breaking cases exceed the threshold (Barthelemy *et al.* 2015*b*; Saket *et al.* 2015) and eventually u_x may overcome V_c (see Figure 3 in Barthelemy *et al.* (2015*b*) and Shemer & Liberzon (2014)). This suggests to look at the space-time transport of wave energy near a large unsteady crest and possible local superharmonic instabilities that are triggered as the threshold B_x is exceeded leading to breaking, as those found for steep steady waves (Longuet-Higgins 1978; Bridges 2004). Our preliminary studies suggest that as a wave crest grows and approaches breaking, the local kinetic energy K_e on the free surface increases much faster than the potential energy $\rho g\zeta$ and the normal kinetic energy flux velocity C_{K_e} tends to reduce approaching the normal fluid velocity speed u_n. Equivalently, the Lagrangian kinetic energy flux speed $C_{K_e} - u_n$ seen by a fluid particle is practically null. Consequently, there is a strong attenuation of accumulation of potential energy on the surface. Thus, at these special instants of time fluid particles on the surface behave like particles in free flight as if the free surface did not exist at all, in agreement with the analysis of the symplectic structure of the particle kinematics. Further studies on the coupling of the kinematics of surface fluid particles with the evolution of the wave field are desirable using Zakharov's (1968) Hamiltonian formalism (Krasitskii (1994); Zakharov (1999)), but these are beyond the scope of this paper.

The Hamiltonian formulation of the JS equations also helps gain significant insight into the possibility of singular behavior of particle trajectories and trapping regions, as conjectured by Bridges (see contributed appendix in Sclavounos (2005)). In particular, exploiting the conservation and special form of the Hamiltonian function for steady surfaces and traveling waves we prove that particle velocities stay bounded at all times, ruling out the possibility of the finite-time blowup of solutions. The same argument does not rule out the possible occurrences of finite-time blowups on unsteady surfaces. We also note that we did not observe any trace of such singular behavior in our numerical simulations of the JS equations with unsteady surfaces (Farazmand *et al.* 2015). We also identify regions where particles are trapped and so remain at all times if their initial velocity is not large enough.

The remainder of the paper is structured as follows. In section 3, we present the physical and mathematical descriptions of vorticity generated on a zero-stress free surface and associated circulation. Then in section 4 we derive the kinematic criterion for wave breaking from the condition of vanishing vorticity at a wave crest. In section 5 the JS

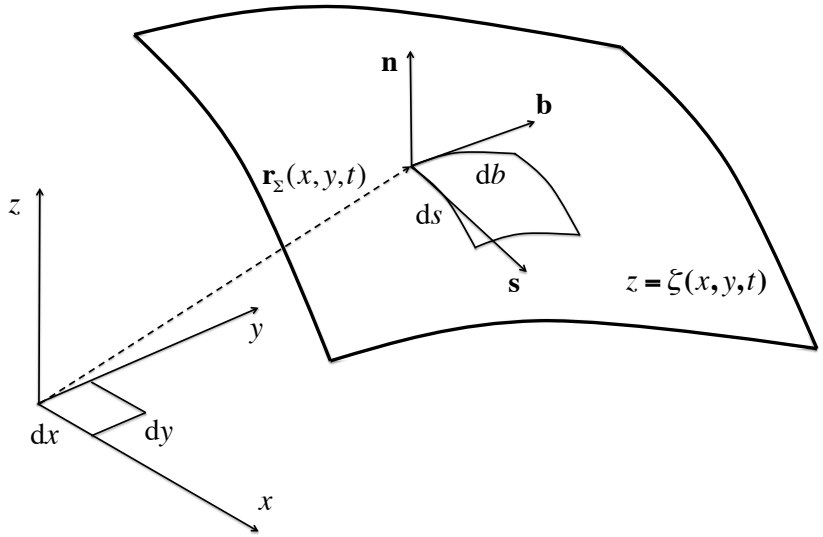

FIGURE 3.1. Reference coordinate system: in the global frame (x, y, z), $\mathbf{r}_\Sigma(x, y, t)$ is a point of the free surface $z = \zeta(x, y, t)$, and $(\mathbf{s}, \mathbf{b}, \mathbf{n})$ is a local frame on the surface.

equations are derived from first principles using a Lagrangian formalism applied to the motion of a frictionless particle constrained on an unsteady surface and subject to gravity. The associated Hamiltonian structure is formulated using Dirac theory and illustrated in section 6. The associated symplectic structure is presented in section 7 and studied in details, with emphasis on the physical interpretation of the one- and two-forms in terms of circulation and vorticity created on the zero-stress free surface. Finally, the finite-time blowup of the JS equations is investigated in section 8 and particle trapping regions are discussed in section 9.

3. Vorticity generated at a zero-stress free surface

In general, vorticity is generated at free surfaces whenever there is flow past regions of surface curvature (Wu 1995; Lundgren & Koumoutsakos 1999). Vorticity is present even if the flow field that generates the curved free-surface is irrotational, and it resides in a vortex sheet along the free-surface if the fluid is inviscid (Longuet-Higgins 1998). The condition of zero shear stress determines the strength of the vorticity at the surface. In the global frame (x, y, z), a point $\mathbf{r}_\Sigma$ of the free-surface Σ can be parametrized as

$$\mathbf{r}_\Sigma(x, y, t) = \begin{pmatrix} x \\ y \\ \zeta(x, y, t) \end{pmatrix},$$

where x and y are the parameters. On the surface consider the local frame $(\mathbf{s}, \mathbf{b}, \mathbf{n})$

$$\mathbf{s} = \frac{\partial_x \mathbf{r}_\Sigma}{|\partial_x \mathbf{r}_\Sigma|}, \qquad \mathbf{b} = \frac{\partial_y \mathbf{r}_\Sigma}{|\partial_y \mathbf{r}_\Sigma|}, \qquad \mathbf{n} = \frac{\partial_x \mathbf{r}_\Sigma \times \partial_y \mathbf{r}_\Sigma}{|\partial_x \mathbf{r}_\Sigma \times \partial_y \mathbf{r}_\Sigma|},$$

where $\mathbf{s}$ and $\mathbf{b}$ are unit vectors tangent to the surface and $\mathbf{n}$ is the unit vector of the outward normal (see Fig. 3.1). More explicitly,

$$\mathbf{s} = \frac{1}{\sqrt{h_1}} \begin{pmatrix} 1 \\ 0 \\ \zeta_x \end{pmatrix}, \qquad \mathbf{b} = \frac{1}{\sqrt{h_2}} \begin{pmatrix} 0 \\ 1 \\ \zeta_y \end{pmatrix}, \qquad \mathbf{n} = \frac{1}{\sqrt{h}} \begin{pmatrix} -\zeta_x \\ -\zeta_y \\ 1 \end{pmatrix}, \tag{3.1}$$

where subscripts of ζ denote partial derivatives with respect to x, y and t,

$$h_1 = |\partial_x \mathbf{r}_\Sigma|^2 = 1 + \zeta_x^2, \qquad h_2 = |\partial_y \mathbf{r}_\Sigma|^2 = 1 + \zeta_y^2,$$

and

$$h = |\partial_x \mathbf{r}_\Sigma \times \partial_y \mathbf{r}_\Sigma|^2 = 1 + \zeta_x^2 + \zeta_y^2.$$

Note that for a 2-D surface, $\mathbf{s}$ and $\mathbf{b}$ are in general not orthogonal as

$$\alpha = \mathbf{s} \cdot \mathbf{b} = \frac{\zeta_x \zeta_y}{\sqrt{h_1 h_2}} \tag{3.2}$$

vanishes only at crests, troughs and saddles. On the surface, we also consider the intrinsic curvilinear cordinates s and b defined as

$$s = \int_0^x \sqrt{h_1(x', y)} \mathrm{d}x', \qquad b = \int_0^y \sqrt{h_2(x, y')} \mathrm{d}y',$$

and the infinitesimal arclengths (see Fig. 1)

$$\mathrm{d}s = \sqrt{h_1} \mathrm{d}x, \qquad \mathrm{d}b = \sqrt{h_2} \mathrm{d}y. \tag{3.3}$$

In the global frame, the horizontal particle velocity components will be denoted, respectively, by

$$u_x = \dot{x}, \qquad u_y = \dot{y}. \tag{3.4}$$

Then, the vertical particle velocity

$$\dot{\zeta} = \frac{d\zeta}{dt} = \zeta_t + \dot{x}\zeta_x + \dot{y}\zeta_y = \zeta_t + u_x \zeta_x + u_y \zeta_y. \tag{3.5}$$

In the global frame, the particle velocity vector

$$\mathbf{u} = u_x \mathbf{i} + u_y \mathbf{j} + \dot{\zeta} \mathbf{k}, \tag{3.6}$$

and in the local frame

$$\mathbf{u} = u_s \mathbf{s} + u_b \mathbf{b} + u_n \mathbf{n}, \tag{3.7}$$

where u_s and u_b are the tangential components to the surface

$$u_s = \frac{U_s - \alpha U_b}{1 - \alpha^2}, \qquad u_b = \frac{U_b - \alpha U_s}{1 - \alpha^2}, \tag{3.8}$$

and

$$u_n = \mathbf{u} \cdot \mathbf{n} = \frac{-\zeta_x u_x - \zeta_y u_y + \dot{\zeta}}{\sqrt{h}} = \frac{\zeta_t}{\sqrt{h}} \tag{3.9}$$

is the normal particle velocity component. Here, U_s and U_b are the projections of $\mathbf{u}$ onto $\mathbf{s}$ and $\mathbf{b}$ respectively, namely

$$U_s = \mathbf{u} \cdot \mathbf{s} = \frac{u_x + \dot{\zeta}\zeta_x}{\sqrt{h_1}} = \frac{(1 + \zeta_x^2) u_x + \zeta_x \zeta_y u_y + \zeta_x \zeta_t}{\sqrt{1 + \zeta_x^2}}, \tag{3.10}$$

$$U_b = \mathbf{u}\cdot\mathbf{b} = \frac{u_y + \dot{\zeta}\zeta_y}{\sqrt{h_2}} = \frac{(1+\zeta_y^2)u_y + \zeta_x\zeta_y u_x + \zeta_y\zeta_t}{\sqrt{1+\zeta_y^2}}. \tag{3.11}$$

Note that the denominators in Eq. (3.8) never vanish as, from Eq. (3.2),

$$1-\alpha^2 = \frac{h}{h_1 h_2} = \frac{1+\zeta_x^2+\zeta_y^2}{(1+\zeta_x^2)\left(1+\zeta_y^2\right)} > 0.$$

Clearly, U_s and U_b coincide with u_s and u_b on the surface when $\mathbf{s}$ and $\mathbf{b}$ are orthogonal, i.e. $\alpha = 0$. Note that u_n vanishes if the surface is steady or in the comoving frame of a traveling wave.

Drawing on Longuet-Higgins (1998), on the assumption of a zero-stress free surface any line of fluid particles parallel to a principal axis of strain must stretch and be in rotation with angular velocity $\frac{1}{2}\boldsymbol{\omega}$, where $\boldsymbol{\omega}$ is the vorticity vector. Since one axis of strain is always normal to the free surface, then the unit normal $\mathbf{n}$ must stretch (or squeeze) and rotate according to

$$\frac{d\mathbf{n}}{dt} = \sigma_n\mathbf{n} + \frac{1}{2}\boldsymbol{\omega}\times\mathbf{n}, \tag{3.12}$$

where σ_n is the eigenvalue of the rate-of-strain tensor $\mathbf{S}$ associated with the eigenvector $\mathbf{n}$, i.e. $\mathbf{S}\mathbf{n} = \sigma_n\mathbf{n}$.

We decompose the vorticity as

$$\boldsymbol{\omega} = \boldsymbol{\omega}_\parallel + \omega_\perp\mathbf{n},$$

into its tangential component $\boldsymbol{\omega}_\parallel$ and its normal component $\omega_\perp\mathbf{n}$ to the surface. Note that

$$\mathbf{n}\times(\boldsymbol{\omega}\times\mathbf{n}) = (\mathbf{n}\cdot\mathbf{n})\,\boldsymbol{\omega} - (\mathbf{n}\cdot\boldsymbol{\omega})\,\mathbf{n} = \boldsymbol{\omega} - \omega_\perp\mathbf{n} = \boldsymbol{\omega}_\parallel, \tag{3.13}$$

gives the vorticity aligned along the surface. The normal vorticity $\omega_\perp\mathbf{n}$ cannot be generated by the surface motion, but it depends upon both the fluid flows above and below the surface. For example, for irrotational and inviscid water wave fields $\omega_\perp = 0$ as there is no discontinuity across the surface since vorticity is divergence-free. However, there is no restriction on the vorticity $\boldsymbol{\omega}_\parallel$ generated by the surface motion, which is indeed discontinuous as it is stored in a vortical sheet along the surface. Then, from Eqs. (3.12) and (3.13) the tangential component $\boldsymbol{\omega}_\parallel$ of vorticity generated on the free surface is given by (Longuet-Higgins (1998))

$$\boldsymbol{\omega}_\parallel = 2\mathbf{n}\times\frac{d\mathbf{n}}{dt}. \tag{3.14}$$

From Eq. (3.1),

$$\frac{d\mathbf{n}}{dt} = \frac{\mathbf{a}}{\sqrt{h}} - \frac{\dot{h}}{2h}\mathbf{n},$$

where

$$\mathbf{a} = -\begin{pmatrix} \partial_x\dot{\zeta} \\ \partial_y\dot{\zeta} \\ 0 \end{pmatrix},$$

$\dot{h} = 2\nabla\zeta \cdot \nabla\dot{\zeta}$ and $\nabla = (\partial_x, \partial_y)$ is the 2-D space gradient. Thus, Eq. (3.14) yields

$$\boldsymbol{\omega}_{\parallel} = 2\mathbf{n} \times \frac{\mathbf{a}}{\sqrt{h}} = \frac{2}{h}\begin{vmatrix} \mathbf{i} & \mathbf{j} & \mathbf{k} \\ -\zeta_x & -\zeta_y & 1 \\ -\partial_x\dot{\zeta} & -\partial_y\dot{\zeta} & 0 \end{vmatrix} = \frac{2}{h}\begin{pmatrix} \partial_y\dot{\zeta} \\ -\partial_x\dot{\zeta} \\ \zeta_x\partial_y\dot{\zeta} - \zeta_y\partial_x\dot{\zeta} \end{pmatrix}, \tag{3.15}$$

where ($\mathbf{i}$,$\mathbf{j}$,$\mathbf{k}$) are the unit vectors along x, y and z respectively. Note that $\boldsymbol{\omega}_{\parallel}$ does not depend on the normal strain σ_n and the z-component ω_3 can be written in the compact form

$$\omega_3 = \boldsymbol{\omega}_{\parallel} \cdot \mathbf{k} = \frac{2}{h}\left(\zeta_x\partial_y\dot{\zeta} - \zeta_y\partial_x\dot{\zeta}\right) = \frac{2}{1+|\nabla\zeta|^2}\nabla\zeta \times \nabla\dot{\zeta}, \tag{3.16}$$

where $\dot{\zeta}$ follows from Eq. (3.5). This observation will be useful later to interpret certain terms of a symplectic 2-form (see Section 6). In the local frame

$$\boldsymbol{\omega}_{\parallel} = \omega_s\mathbf{s} + \omega_b\mathbf{b}, \tag{3.17}$$

where

$$\omega_s = \frac{\Omega_s - \alpha\Omega_b}{1-\alpha^2}, \qquad \omega_b = \frac{\Omega_b - \alpha\Omega_s}{1-\alpha^2}, \tag{3.18}$$

and Ω_s and Ω_b are the projections of $\boldsymbol{\omega}_{\parallel}$ onto $\mathbf{s}$ and $\mathbf{b}$ respectively, that is

$$\Omega_s = \boldsymbol{\omega}_{\parallel}\cdot\mathbf{s} = 2\frac{\sqrt{h_1}\partial_y\dot{\zeta} - \alpha\sqrt{h_2}\partial_x\dot{\zeta}}{h} \tag{3.19}$$

and

$$\Omega_b = \boldsymbol{\omega}_{\parallel}\cdot\mathbf{b} = -2\frac{\sqrt{h_2}\partial_x\dot{\zeta} - \alpha\sqrt{h_1}\partial_y\dot{\zeta}}{h}. \tag{3.20}$$

On the surface where $\mathbf{s}$ and $\mathbf{b}$ are orthogonal, i.e. $\alpha = 0$, Ω_s and Ω_b coincide with ω_s and ω_b respectively.

Vorticity created on the free-surface Σ implies that there is non-zero circulation of the velocity $\mathbf{u} = (u_x, u_y, \dot{\zeta})$ along any closed path $\gamma(\mu, t) = (x(\mu, t), y(\mu, t), \zeta(x(\mu, t), y(\mu, t)))$ on Σ, parametrized by μ, and it is conserved by Kelvin's theorem (see, e.g., Eyink (2007)). From Eqs. (3.5) and $\mathrm{d}z = \zeta_x\mathrm{d}x + \zeta_y\mathrm{d}y$, the circulation around γ

$$\oint_{\gamma(t)} \mathbf{u}\cdot\mathbf{dx} = \oint_{\gamma(t)} u_x\mathrm{d}x + u_y\mathrm{d}y + \dot{\zeta}\mathrm{d}z, \tag{3.21}$$

can be expressed in terms of the projections U_s and U_b of the particle velocity $\mathbf{u}$ as [see Eqs. (3.10) and (3.11)]

$$\oint_{\gamma(t)} \mathbf{u}\cdot\mathbf{dx} = \oint_{\widetilde{\gamma}(t)} \sqrt{h_1}U_s\mathrm{d}x + \sqrt{h_2}U_b\mathrm{d}y = \oint_{\widetilde{\widetilde{\gamma}}(t)} U_s\mathrm{d}s + U_b\mathrm{d}b, \tag{3.22}$$

where we have used Eq. (3.3), and $\widetilde{\gamma}(t) = (x(\mu, t), y(\mu, t))$ and $\widetilde{\widetilde{\gamma}}(t) = (s(\mu, t), b(\mu, t))$ are the projected paths of γ onto the x, y and s, b planes respectively.

4. Kinematic criterion for wave breaking

Consider now the special case of unidirectional waves propagating along x and the associated 1-D surface $z = \zeta(x, t)$. In this case, $\mathbf{b} = \mathbf{j}$ is aligned along y and orthogonal

to **s** (see Fig. 1). Then, from Eq. (3.18) vorticity created on the surface is aligned along y and it is given by

$$\omega_b = \Omega_b = -\frac{2}{h_1}\partial_x\dot{\zeta} = \frac{2}{h_1}\left(\zeta_{xt} + u_x\zeta_{xx}\right). \tag{4.1}$$

This can be written as (Lundgren & Koumoutsakos (1999))

$$\omega_b = -2\left(\frac{\mathrm{d}u_n}{\mathrm{d}s} + u_s K\right), \tag{4.2}$$

where

$$K = \frac{\zeta_{xx}}{h_1^{3/2}} = \frac{\zeta_{xx}}{(1+\zeta_x^2)^{3/2}},$$

is the surface curvature. The tangential particle velocity u_s follows from Eq. (3.10) as

$$u_s = U_s = \frac{h_1 u_x + \zeta_x\zeta_t}{\sqrt{h_1}},$$

and the rate of change of the normal particle velocity $u_n = \zeta_t/\sqrt{h_1}$ along the intrinsic curvilinear cordinates s on the surface is given by

$$\frac{\mathrm{d}u_n}{\mathrm{d}s} = \frac{\mathrm{d}u_n}{\mathrm{d}x}\frac{\mathrm{d}x}{\mathrm{d}s} = \frac{\zeta_{xt}}{h_1} - \frac{\zeta_t\zeta_x\zeta_{xx}}{h_1^2},$$

where the infinitesimal arclength $\mathrm{d}s = \sqrt{h_1}\mathrm{d}x$ [see Eq. (3.3)]. For steady surfaces $u_n = 0$ and Eq. (4.2) reduces to Longuet-Higgins' (1988) result

$$\omega_b = -2u_s K.$$

Thus, in a comoving frame where travelling waves are steady, at crests vorticity is positive or counter-clockwise (Longuet-Higgins (1992)). For unsteady surfaces the normal velocity u_n does not vanish as it balances the underneath horizontal water flow leading to convergence (growing crests) or divergence (decaying crests). In particular, at a crest of a wave $\frac{\mathrm{d}u_n}{\mathrm{d}s} > 0$ since the wave travels forward as a result of the downward (upward) mass flow before (after) the crest. Thus, the convergence/divergence of the flow induced by unsteady surfaces creates negative vorticity that can counterbalance that generated by the surface curvature. Indeed, from Eq. (4.1) vorticity vanishes at a crest, where $\zeta_x = 0$, when

$$\zeta_{xt} + u_x\zeta_{xx} = 0. \tag{4.3}$$

A physical interpretation of this condition is as follows: Consider the horizontal speed $V_c = \dot{X}_c$ of a crest and $X_c(t)$ is the horizontal crest location. Since $\zeta_x = 0$ at a crest, then (Fedele 2014)

$$\frac{\mathrm{d}}{\mathrm{d}t}\zeta_x(X_c(t),t) = \zeta_{xt} + \dot{X}_c\zeta_x = 0,$$

from which

$$V_c = \dot{X}_c = -\frac{\zeta_{xt}}{\zeta_{xx}}. \tag{4.4}$$

Thus, condition (4.3) of vanishing vorticity holds when

$$u_x = V_c, \tag{4.5}$$

or equivalently when the horizontal particle velocity u_x equals the horizontal crest speed V_c. Furthermore, from Eq. (3.17) vorticity created on a 2-D surface vanishes when

$$\zeta_{xt} + u_x\zeta_{xx} + u_y\zeta_{xy} = 0, \qquad \zeta_{yt} + u_x\zeta_{xy} + u_y\zeta_{yy} = 0, \tag{4.6}$$

or equivalently when the horizontal particle velocity $\mathbf{u}_h = (u_x, u_y)$ equals the horizontal crest speed $\mathbf{V}_c = (\dot{X}_c, \dot{Y}_c)$, where $(X_c(t), Y_c(t))$ is the horizontal crest position. At a crest where $\nabla\zeta = \mathbf{0}$

$$\frac{\mathrm{d}}{\mathrm{d}t}\nabla\zeta\left(X_c(t), Y_c(t), t\right) = \nabla\dot{\zeta} = \mathbf{0},$$

or equivalently

$$\zeta_{xt} + \dot{X}_c\zeta_{xx} + \dot{Y}_c\zeta_{xy} = 0, \qquad \zeta_{yt} + \dot{X}_c\zeta_{xy} + \dot{Y}_c\zeta_{yy} = 0. \tag{4.7}$$

Clearly, Eq. (4.7) reduces to condition (4.6) of vanishing vorticity if

$$\mathbf{u}_h = \mathbf{V}_c. \tag{4.8}$$

Equations (4.5) and (4.8) are the kinematic thresholds defined as potential breaking criteria for uni- and multidirectional water waves (see, for example Perlin *et al.* (2013)). In particular, recent experimental results by Shemer & Liberzon (2014) and Shemer & Ee (2015) showed that as the largest crest of a focusing wave group grows in time the crest speed decreases, while water particles at the crest accelerate. Spilling breakers appear to occur when the horizontal particle velocity exceeds the crest speed, thus confirming the kinematic criterion for the inception of wave breaking (see also Shemer (2013); Qiao & Duncan (2001); Duncan *et al.* (1999)). Further, Qiao & Duncan (2001) showed that as the particle velocity exceeds the crest speed a volume (bulge) of water near the crest is shifted towards the forward face of the wave and (negative or clockwise) vorticity is generated within the bulge. Longuet-Higgins & Cleaver (1994) showed that the one unstable normal-mode perturbation of the almost-highest wave resembles the initial stage flow of spilling breakers. Here, the almost-highest wave is the asymptotic form of a very sharp but rounded crest of a steep, irrotational gravity wave that approaches the limiting steady Stokes corner flow with a sharp angle of 120° (Longuet-Higgins & Fox 1977, 1978). However, the actual flow of a breaking wave is unsteady and it is believed that the steady Stokes limiting form is by-passed, with breaking occurring at smaller steepness then the limiting Stokes value of 0.443 in deep water (see Banner & Peregrine (1993) and references therein).

Recent studies point at the crest slowdown as what appears to be the underlying inviscid mechanism from which breaking onset initiates. In particular, the multifaceted study by Banner *et al.* (2014) on unsteady highly nonlinear wave packets highlights the existence a generic oscillatory crest leaning mode that leads to a systematic crest speed slowdown of $\sim 20\%$ lower than the linear phase speed at the dominant wavelength (Fedele 2014). This explains why initial breaking wave crest speeds are observed to be $\sim 80\%$ of the linear carrier-wave speed (Rapp & Melville (1990); Stansell & MacFarlane (2002)).

Clearly, both the particle kinematics on the free surface and the energetics of the wave field that generates the surface should be considered to establish if the kinematic criterion for incipient breaking is valid. Recent studies show that the breaking onset of the largest crest of unsteady wave groups initiates before the particle velocity u_x reaches the crest speed value V_c, i.e. when it exceeds about 0.84 times the crest velocity (Barthelemy *et al.* (2015*b*); Saket *et al.* (2015), see also Kurnia & van Groesen (2014)). In particular, none of the recurrent groups reach the threshold $B_x = u_x/V_c = 0.84$, while all marginal breaking cases exceed the threshold. Furthermore, Song & Banner (2002) and more recently Barthelemy *et al.* (2015*b*) explored the existence of an energy flux threshold related to the breaking onset. This suggests to look at the space-time transport of wave energy fluxes near a large crest of an unsteady wave group and possible

local superharmonic instabilities that initiate as the threshold B_x is exceeded leading to breaking, as those found for steady steep waves (Longuet-Higgins 1978).

In the following we present an explorative study of the wave energy transport below a crest and the relation to the crest slowdown. Clearly, such study is not exhaustive as it requires further analysis and thinking that are beyond the scope of this paper. The irrotational Eulerian velocity field $\mathbf{U} = (U, V, W) = (\phi_x, \phi_y, \phi_z)$ that generates the free surface ζ is given by the gradient of the potential ϕ, where the subscript in $\phi_x = \partial_x \phi$ denotes partial differentiation. Clearly, from Eq. (3.6) the velocity $\mathbf{u} = (u_x, u_y, u_z)$ of a fluid particle that at time t passes through the point $\mathbf{x}_P$ is $\mathbf{u}(t) = \mathbf{U}(\mathbf{x}_P, t)$. Besides the Laplace equation to impose fluid incompressibility in the flow domain, ϕ satisfies the dynamic Bernoulli and kinematic conditions on the free surface (see, e.g Zakharov (1968, 1999))

$$\rho\phi_t + \rho g\zeta + K_e = 0, \qquad z = \zeta, \tag{4.9}$$

and

$$\phi_z = \zeta_t + U\zeta_x + V\zeta_y, \qquad z = \zeta, \tag{4.10}$$

where $K_e = \rho|\mathbf{U}|^2/2$ is the kinetic energy density. Drawing on Tulin (2007), consider the transport equation

$$\partial_t K_e + \nabla \cdot \mathbf{F}_{K_e} = 0 \tag{4.11}$$

and the associated flux

$$\mathbf{F}_{K_e} = -\rho\phi_t \mathbf{U}. \tag{4.12}$$

Equation (4.11) can be written as

$$\partial_t K_e + \nabla \cdot (\mathbf{C}_{K_e} K_e) = 0, \tag{4.13}$$

where we have defined the Eulerian kinetic energy flux velocity

$$\mathbf{C}_{K_e} = \frac{\mathbf{F}_{K_e}}{K_e} = -\frac{\rho\phi_t}{K_e}\mathbf{U}. \tag{4.14}$$

At the free-surface, the kinetic energy flux in Eq. (4.12) can be written as

$$\mathbf{f}_{K_e} = \mathbf{U}\left(\rho g\zeta + K_e\right), \qquad z = \zeta, \tag{4.15}$$

where we have used the Bernoulli equation (4.9). Then, the rate of change of the surface potential energy density $P_e = \rho g\zeta^2/2$ (Tulin 2007)

$$\partial_t P_e = \mathbf{f}_{K_e} \cdot \mathbf{n}/\cos\theta \tag{4.16}$$

is due to the flux of kinetic energy into the moving interface ζ

$$\mathbf{f}_{K_e} \cdot \mathbf{n} = U_n\left(\rho g\zeta + K_e\right) \qquad z = \zeta, \tag{4.17}$$

where $U_n = \mathbf{U} \cdot \mathbf{n}$ is the fluid velocity normal to the surface and θ the angle between $\mathbf{n}$ and the vertical (at a wave crest, $\theta = 0$). The sum of the total kinetic energy K_e integrated over the wave domain and the potential energy P_e integrated over the surface is conserved. Clearly, a wave crest grows when the adjacent kinetic energy flux behind the crest is larger than the flux after the crest.

For unidirectional waves, the kinematic condition (4.10) reduces to

$$\zeta_t = W - U\zeta_x,$$

and

$$\zeta_{xt} = \partial_x W - \partial_x U\zeta_x - \partial_z W\zeta_x^2 - U\zeta_{xx},$$

Then, at $\zeta_x = 0$ the crest speed in Eq. (4.4) can be written as

$$V_c = -\frac{\zeta_{yt}}{\zeta_{xx}} = U - \frac{\partial_x W}{\zeta_{xx}} = U - \frac{\partial_z U}{\zeta_{xx}}, \tag{4.18}$$

where $\partial_x W = \partial_z U$ because of irrotationality. At a crest $\zeta_{xx} < 0$ and the vertical gradient $\partial_z U > 0$ as indicated by measurements and simulations (Barthelemy *et al.* 2015*a*,*b*). As a result, for smooth wave fields the crest speed V_c is always larger than the horizontal fluid velocity U. According to Eq. (4.18), only when crest becomes steep ($|\zeta_{xx}| \gg 1$) or the horizontal velocity profile flattens near the crest ($\partial_z U \ll 1$) is the crest speed V_c closer to the particle speed $u_x = U$. Thus, the observation that the initiation of breaking occurs when V_c is actually 0.84 times the particle speed is the kinematic manifestation of the space-time transport of kinetic energy below the crest (Barthelemy *et al.* 2015*b*; Saket *et al.* 2015). Indeed, from Eq. (4.17) the normal velocity C_{K_e} of kinetic energy into the moving surface is given by

$$C_{K_e} = \frac{\mathbf{f}_{K_e} \cdot \mathbf{n}}{K_e} = U_n \left(1 + \frac{\rho g \zeta}{K_e}\right). \tag{4.19}$$

Note that C_{K_e} is always larger than the fluid speed U_n normal to the surface. However, we expect that as the wave crest grows reaching nearly breaking the local kinetic energy K_e increases much faster than the potential energy $\rho g \zeta$ and C_{K_e} tends to U_n and the accumulation of potential energy into the surface is largerly attenuated. Equivalently, the Lagrangian kinetic energy flux speed $C_{K_e} - U_n$ seen by fluid particles on the surface is practically null. Near such conditions, fluid particles on the free surface behave like particles in free flight as if the free surface did not exist. The symplectic structure of the particle kinematics on the sea surface will lead to the same conclusions as it will be shown later.

In the following, we will derive the JS equations from first principles using Lagrangian and Hamiltonian formalisms applied to the constrained motion of a frictionless particle on an unsteady surface.

5. Lagrangian formalism

The Lagrangian for a free particle subject to gravity in $\mathbb{R}^3$ is given by

$$\mathcal{L}(\mathbf{r}, \dot{\mathbf{r}}) = K - P,$$

where the kinetic and potential energies

$$K = \frac{1}{2}\left(\dot{x}^2 + \dot{y}^2 + \dot{z}^2\right), \qquad P = gz,$$

and $\mathbf{r} = (x(t), y(t), z(t))$ is the instantaneous vector particle position. Minimizing the action $\mathcal{A} = \int \mathcal{L} dt$ over all possible paths yields the Euler–Lagrange equations

$$\frac{\delta \mathcal{A}}{\delta \mathbf{r}} = \frac{d}{dt}\left(\frac{\partial \mathcal{L}}{\partial \dot{\mathbf{r}}}\right) - \frac{\partial \mathcal{L}}{\partial \mathbf{r}} = 0,$$

or equivalently, $\ddot{\mathbf{r}} = \mathbf{f}$, where $\mathbf{f} = (0, 0, -g)$.

We now assume that the particle is constrained to move on an unsteady surface $z = \zeta(x, y, t)$. Thus, the horizontal particle motion is coupled with that of the evolving surface. The associated dynamical equations follow from the constrained Lagrangian

$$\mathcal{L}_c = \mathcal{L} + \lambda\left[z - \zeta(x, y, t)\right], \tag{5.1}$$

where we have introduced the Lagrange multiplier $\lambda = \lambda(x, y, t)$ to impose that the particle always stays on the surface $z = \zeta$. Minimizing the action with respect to x, y, z and λ yields the set of Euler–Lagrange equations

$$\frac{d}{dt}\frac{\partial \mathcal{L}_\mathrm{c}}{\partial \dot{x}} - \frac{\partial \mathcal{L}_\mathrm{c}}{\partial x} = \ddot{x} - \lambda_x(z-\zeta) + \lambda\zeta_x = 0, \tag{5.2}$$

$$\frac{d}{dt}\frac{\partial \mathcal{L}_\mathrm{c}}{\partial \dot{y}} - \frac{\partial \mathcal{L}_\mathrm{c}}{\partial y} = \ddot{y} - \lambda_y(z-\zeta) + \lambda\zeta_y = 0, \tag{5.3}$$

$$\frac{d}{dt}\frac{\partial \mathcal{L}_\mathrm{c}}{\partial \dot{z}} - \frac{\partial \mathcal{L}_\mathrm{c}}{\partial z} = \ddot{z} + \mathrm{g} - \lambda = 0, \tag{5.4}$$

$$\frac{\partial \mathcal{L}_\mathrm{c}}{\partial \lambda} = z - \zeta = 0. \tag{5.5}$$

Here, the last equation imposes the constraint $z = \zeta$, which can be differentiated twice with respect to time to yield the vertical particle velocity

$$\dot{z} = \zeta_x\dot{x} + \zeta_y\dot{y} + \zeta_t, \tag{5.6}$$

and acceleration

$$\ddot{z} = \zeta_x\ddot{x} + \zeta_y\ddot{y} + \zeta_{xt}\dot{x} + \zeta_{yt}\dot{y} + \zeta_{xx}\dot{x}^2 + 2\zeta_{xy}\dot{x}\dot{y} + \zeta_{yy}\dot{y}^2 + \zeta_{tt},$$

as a function of the horizontal variables $(x, y, \dot{x}, \dot{y})$. Then, from Eqs. (5.2)-(5.3) the horizontal trajectories satisfy the coupled ordinary differential equations (ODEs)

$$\begin{aligned} \ddot{x} + \lambda\zeta_x &= 0, \\ \ddot{y} + \lambda\zeta_y &= 0. \end{aligned} \tag{5.7}$$

The multiplier λ follows from Eq. (5.4) as

$$\lambda = \ddot{z} + \mathrm{g}.$$

As a result, Eqs. (5.7) can be written as

$$\ddot{x} + (\ddot{z} + \mathrm{g})\,\zeta_x = 0,$$

$$\ddot{y} + (\ddot{z} + \mathrm{g})\,\zeta_y = 0,$$

which are identical to the JS equations [see Eqs. (2.17)-(2.18) in Sclavounos (2005)]:

$$\begin{aligned} &\left(1+\zeta_x^2\right)\ddot{x} + \zeta_x\zeta_y\ddot{y} + \left(\zeta_{tt} + \zeta_{xt}\dot{x} + \zeta_{yt}\dot{y} + \zeta_{xx}\dot{x}^2 + 2\zeta_{xy}\dot{x}\dot{y} + \zeta_{yy}\dot{y}^2 + \mathrm{g}\right)\zeta_x = 0, \\ &\left(1+\zeta_y^2\right)\ddot{y} + \zeta_x\zeta_y\ddot{x} + \left(\zeta_{tt} + \zeta_{xt}\dot{x} + \zeta_{yt}\dot{y} + \zeta_{xx}\dot{x}^2 + 2\zeta_{xy}\dot{x}\dot{y} + \zeta_{yy}\dot{y}^2 + \mathrm{g}\right)\zeta_y = 0. \end{aligned} \tag{5.8}$$

The JS equations can also be obtained by minimizing the action associated with the reduced Lagrangian

$$\widetilde{\mathcal{L}}_c = \frac{1}{2}\left(\dot{x}^2 + \dot{y}^2 + (\zeta_t + \zeta_x\dot{x} + \zeta_y\dot{y})^2\right) - \mathrm{g}\zeta,$$

which follows from the augmented Lagrangian in Eq. (5.1) setting $z = \zeta$ and $\dot{z}$ equal to Eq. (5.6). In matrix form

$$\widetilde{\mathcal{L}}_c = \frac{1}{2}\dot{\mathbf{x}}^T\mathbf{B}\dot{\mathbf{x}} + \boldsymbol{\alpha}^T\dot{\mathbf{x}} - \mathrm{g}\zeta + \frac{1}{2}\zeta_t^2,$$

where $\mathbf{x} = (x(t), y(t))$ is the horizontal vector of position and

$$\mathbf{B} = \begin{bmatrix} 1+\zeta_x^2 & \zeta_x\zeta_y \\ \zeta_x\zeta_y & 1+\zeta_y^2 \end{bmatrix}, \qquad \boldsymbol{\alpha} = \zeta_t\begin{bmatrix} \zeta_x \\ \zeta_y \end{bmatrix}. \tag{5.9}$$

We note that $\mathbf{B}$ is symmetric and positive-definite with real eigenvalues

$$\lambda_1 = 1, \qquad \lambda_2 = |\mathbf{B}| = 1 + \zeta_x^2 + \zeta_y^2,$$

and the corresponding orthogonal eigenvectors

$$\mathbf{w}_1 = (-\zeta_y, \zeta_x) = \nabla^\perp \zeta, \qquad \mathbf{w}_2 = (\zeta_x, \zeta_y) = \nabla \zeta.$$

These will be useful later in the analysis of the finite time blowup of the JS equations (cf. Section 8).

The generalized momentum $\mathbf{p} = (p_x, p_y)$ is a function of the horizontal particle velocity $\dot{\mathbf{x}}$ as

$$\mathbf{p} = \mathbf{B}\dot{\mathbf{x}} + \boldsymbol{\alpha}, \tag{5.10}$$

where

$$p_x = \frac{\partial \widetilde{\mathcal{L}}_c}{\partial \dot{x}} = \left(1 + \zeta_x^2\right) \dot{x} + \zeta_x \zeta_y \dot{y} + \zeta_x \zeta_t, \tag{5.11}$$

and

$$p_y = \frac{\partial \widetilde{\mathcal{L}}_c}{\partial \dot{y}} = \left(1 + \zeta_y^2\right) \dot{y} + \zeta_y \zeta_x \dot{x} + \zeta_y \zeta_t. \tag{5.12}$$

Then $(\mathbf{p}, \mathbf{x})$ are canonically conjugate variables and the Hamiltonian follows from the Legendre transform of $\widetilde{\mathcal{L}}$ as (Morrison 1998)

$$\mathcal{H}_c = p_x \dot{x} + p_y \dot{y} - \widetilde{\mathcal{L}} = \mathbf{p}^T \dot{\mathbf{x}} - \widetilde{\mathcal{L}}. \tag{5.13}$$

From Eq. (5.10) the horizontal particle velocity $\dot{\mathbf{x}}$ can be written as a function of the canonical momentum $\mathbf{p}$, and the Hamiltonian can be recast as

$$\mathcal{H}_c = \frac{1}{2} \left(\mathbf{p} - \boldsymbol{\alpha}\right)^T \mathbf{B}^{-1} \left(\mathbf{p} - \boldsymbol{\alpha}\right) + \mathrm{g}\zeta - \frac{1}{2}\zeta_t^2. \tag{5.14}$$

Note that for unsteady surfaces, $\mathcal{H}_c$ is not time-invariant as particles behave as an open system exchanging energy with the moving surface.

Comparing Eqs. (5.11), (5.12) with Eqs. (3.10), (3.11), we note that the infinitesimal circulation in Eq. (3.22) can be written in terms of generalized momenta as

$$U_s \mathrm{d}s + U_b \mathrm{d}b = p_x \mathrm{d}x + p_y \mathrm{d}y, \tag{5.15}$$

where the arclengths $\mathrm{d}s$ and $\mathrm{d}b$ relate to $\mathrm{d}x$ and $\mathrm{d}y$ via Eq. (3.3). Thus, the scaled generalized momenta $(p_x/\sqrt{h_1}, p_y/\sqrt{h_2})$ are equal to the particle velocity projections (U_s, U_b).

The Lagrangian formalism developed above highlights a fundamental property of the JS equations. On the one hand, these are originally derived from the dynamical condition that the zero-stress free surface $z = \zeta$ is an iso-pressure surface (Sclavounos 2005). On the other hand, we have derived the same equations from an action principle for the constrained motion of a frictionless particle subject to gravity on an unsteady surface. The unsteady surface is arbitrary and can be generated by many physical processes. If the interest is in the kinematics of fluid particles on the free surface of gravity water waves, one must know the irrotational velocity field beneath the waves. Indeed, only if the initial particle velocity is set as that induced by the irrotational flow do the JS equations describe the kinematics of fluid particles.

A rigorous proof of the previous statement is beyond the scope of this paper. We only point out that the horizontal velocity $\dot{\mathbf{x}}$ of a fluid particle on an irrotational water surface satisfies

$$\dot{\mathbf{x}} = \mathbf{U}_h(\mathbf{x}(t), \zeta(x, y, t), t), \tag{5.16}$$

where the horizontal Eulerian velocity $\mathbf{U}_h = \nabla\phi = (\phi_x, \phi_y)$ is given in terms of the velocity potential $\phi(x, y, z, t)$. Thus, we expect that the JS equations (5.8) can also be derived using Eq. (5.16) and the Stokes equations in Eqs. (4.9), (4.10) (see Appendix A for the case of steady irrotational flows).

6. Hamiltonian formalism via Dirac Theory

The Lagrangian formalism developed in the previous section yields the Hamiltonian structure of the JS equations (5.8) in terms of the canonical variables $(\mathbf{p}, \mathbf{x})$. A non-canonical structure in terms of the original physical variables (position $\mathbf{x}$ and velocity $\mathbf{u}$) can be derived within the framework of Dirac's (1950) theory of constrained Hamiltonian systems (see also Dirac (1958)). The transformation (5.10) between the non-canonical and canonical variables follows from Darboux's theorem (see, e.g Morrison (1998)).

6.1. *Dirac theory: an overview*

Consider a parent (unconstrained) Hamiltonian system defined by the Poisson bracket

$$\{F, G\} = \nabla F \cdot \mathbb{J}(\mathbf{z})\nabla G, \tag{6.1}$$

and Hamiltonian $\mathcal{H}(\mathbf{z})$ with dynamical variables $\mathbf{z} = (z_1, \ldots, z_N)$, where $\mathbb{J}(\mathbf{z})$ is the $N \times N$ Poisson matrix and $\nabla = (\partial_{z_1}, \ldots, \partial_{z_N})$. We recall that the Poisson bracket is an antisymmetric bilinear operator, which satisfies the Leibniz rule

$$\{F_1F_2, F_3\} = F_1\{F_2, F_3\} + \{F_1, F_3\}F_2,$$

and the Jacobi identity

$$\{\{F_1, F_2\}, F_3\} + \{\{F_3, F_1\}, F_2\} + \{\{F_2, F_3\}, F_1\} = 0,$$

for all observables $F_1(\mathbf{z})$, $F_2(\mathbf{z})$ and $F_3(\mathbf{z})$, which are scalar functions of the dynamical variables.

Now impose that the dynamical variables satisfy the set of constraints $\Phi_\alpha(\mathbf{z}) = 0$ for $\alpha = 1, \ldots, K$. Then, following Dirac (1950, 1958) the Dirac bracket $\{\cdot, \cdot\}$ of the constrained Hamiltonian system is written as

$$\{F, G\}_* = \{F, G\} - \{F, \Phi_\alpha\}D_{\alpha\beta}\{\Phi_\beta, G\}.$$

Here, the $K \times K$ matrix $\mathbb{D}$ with elements $D_{\alpha\beta}$ is defined such that the K constraints are Casimir invariants of the Dirac bracket, i.e. $\{F, \Phi_\alpha\}_* = 0$ for all observables F. As a result, the Dirac bracket is a Poisson bracket that satisfies the Jacobi identity (Chandre 2013). Furthermore, if the $K \times K$ matrix $\mathbb{C}$ with entries

$$C_{\alpha\beta} = \{\Phi_\alpha, \Phi_\beta\},$$

is invertible, then (Dirac (1950, 1958))

$$\mathbb{D} = \mathbb{C}^{-1}. \tag{6.2}$$

Then, the Dirac bracket

$$\{F, G\}_* = \nabla F \cdot \mathbb{J}_*\nabla G, \tag{6.3}$$

is the same as the parent (unconstrained) Poisson bracket in Eq. (6.1) except that $\mathbb{J}$ is replaced with

$$\mathbb{J}_* = \mathbb{J} - \mathbb{J}\hat{\mathcal{Q}}^\dagger\mathbb{D}\hat{\mathcal{Q}}\mathbb{J}, \tag{6.4}$$

where the $K \times N$ matrix $\hat{\mathcal{Q}}$ has elements

$$\hat{\mathcal{Q}}_{\alpha l} = \frac{\partial \Phi_\alpha}{\partial z_l},$$

and † denotes Hermitian transposition. Since $\mathbb{C} = \hat{\mathcal{Q}}\mathbb{J}\hat{\mathcal{Q}}^\dagger$, the Poisson matrix of the Dirac bracket can be computed algebraically by way of a projector (Chandre *et al.* 2013)

$$\mathcal{P}_* = \mathbb{I}_N - \hat{\mathcal{Q}}^\dagger \mathbb{D} \hat{\mathcal{Q}} \mathbb{J},$$

where $\mathbb{I}_N$ is the $N \times N$ identity matrix. If $\mathbb{C}$ is invertible, $\mathcal{P}_* \hat{\mathcal{Q}}^\dagger = 0$, which is an alternative way to characterize constraints that are Casimir invariants. The Dirac projector $\mathcal{P}_*$ projects the dynamics onto the surface defined by the constraints. The expression of $\mathbb{J}_*$ is given by $\mathbb{J}_* = \mathbb{J}\mathcal{P}_* = \mathcal{P}_*^\dagger \mathbb{J} \mathcal{P}_*$. This provides a systematic and straightforward procedure to compute Dirac brackets.

In this procedure the Hamiltonian is not changed, meaning that the equations of motion for the constrained dynamics are given by

$$\dot{F} = \{F, \mathcal{H}\}_*,$$

where F is any dynamical variable (or any function of the dynamical variables) and the Dirac bracket is that in Eq. (6.3).

6.2. *Non-canonical Hamiltonian of the JS equations*

Consider the motion of a free particle in $\mathbb{R}^3$ as a parent model and (x, u_x), (y, u_y) and (z, u_z) are canonically conjugate variables with the standard Poisson bracket

$$\{F, G\} = \nabla F \cdot \overline{\mathbb{J}} \nabla G,$$

where $\mathbf{z} = (x, y, z, u_x, u_y, u_z)$ are the dynamical variables and the Poisson matrix

$$\overline{\mathbb{J}} = \begin{pmatrix} 0 & \mathbb{I}_4 \\ -\mathbb{I}_4 & 0 \end{pmatrix}.$$

We wish to constrain the particle motion on the moving surface $z = \zeta(x, y, t)$. Since this constraint depends explicitly on time, we first autonomize the system adding a pair of canonically conjugate variables (t, E), where E is the energy exchanged by the particle with the moving surface. Indeed, the particle behaves as an open system if the motion is on unsteady surfaces. Constraints are only function of the dynamical variables

$$\overline{\mathbf{z}} = (x, y, z, t, u_x, u_y, u_z, E),$$

as required by Dirac's theory, and $\overline{\mathbf{z}}(\tau)$ is a generic trajectory in the extended phase space, parametrized by τ which plays the role of time for the autonomous system. The associated Hamiltonian is

$$\overline{\mathcal{H}} = \frac{u_x^2 + u_y^2 + u_z^2}{2} + \mathrm{g}z + E.$$

Following Dirac (1958), we now impose as a primary constraint $\Phi_1 = 0$ that the particle must be on the moving surface $z = \zeta$. The secondary constraint $\Phi_2 = 0$ follows by imposing that the vertical particle velocity $u_z = \dot{z}$ equals $\mathrm{d}\zeta/\mathrm{d}t$, or equivalently $\mathrm{d}(z - \zeta(x, y, t))/\mathrm{d}t = 0$. Then,

$$\Phi_1 = z - \zeta(x, y, t) = 0, \qquad \Phi_2 = u_z - u_x \zeta_x - u_y \zeta_y - \zeta_t = 0. \tag{6.5}$$

From Eq. (6.2), the 2×2 matrix $\mathbb{D}$ follows from the inverse of the symplectic matrix $\mathbb{C} = [C_{\alpha\beta}]$ with entries

$$C_{11} = C_{22} = 0, \qquad C_{12} = -C_{21} = \{\Phi_1, \Phi_2\} = 1 + \zeta_x^2 + \zeta_y^2,$$

where the Poisson bracket $\{F, G\}$ is that of the parent (unconstrained) system in Eq. (6.1). Since C_{12} is always non-zero, $\mathbb{C}$ is invertible. The Poisson matrix associated with the Dirac bracket is computed from Eq. (6.4). The resulting Poisson matrix does not explicitly depend on z and u_z. As a consequence, the Poisson bracket of two functions of (x, y, t, u_x, u_y, E) is again a function of (x, y, t, u_x, u_y, E). In other words, the algebra of observables $F(x, y, t, u_x, u_y, E)$ is a Poisson sub-algebra. In this way, one can omit z and u_z (since their dynamics is quite trivially given by the constraints which are Casimir invariants of the Dirac bracket) and the phase-space dimension is reduced by two. The associated Poisson matrix $\overline{\mathbb{J}}_*$ is now a 6×6 matrix

$$\overline{\mathbb{J}}_* = \begin{pmatrix} 0 & \overline{\mathbf{B}}^{-1} \\ -(\overline{\mathbf{B}}^{-1})^T & \overline{\mathcal{B}} \end{pmatrix}, \tag{6.6}$$

where

$$\overline{\mathbf{B}} = \begin{pmatrix} 1+\zeta_x^2 & \zeta_x\zeta_y & \zeta_x\zeta_t \\ \zeta_x\zeta_y & 1+\zeta_y^2 & \zeta_y\zeta_t \\ 0 & 0 & 1 \end{pmatrix},$$

and

$$\overline{\mathcal{B}} = \begin{pmatrix} 0 & -b_3 & b_2 \\ b_3 & 0 & -b_1 \\ -b_2 & b_1 & 0 \end{pmatrix},$$

with the vector $\mathbf{b}_{\mathrm{m}} = (b_1, b_2, b_3)$ given by

$$\mathbf{b}_{\mathrm{m}} = \frac{\overline{\nabla}\zeta \times \overline{\nabla}\left(u_x\zeta_x + u_y\zeta_y + \zeta_t\right)}{1 + |\nabla\zeta|^2} = \frac{\overline{\nabla}\zeta \times \left[\left(\overline{u} \cdot \overline{\nabla}\right)\overline{\nabla}\zeta\right]}{1 + |\nabla\zeta|^2}. \tag{6.7}$$

Here $\overline{\nabla}$ designates the gradient in space-time variables (x, y, t) whereas ∇ is the gradient in space variables (x, y) and $\overline{u} = (u_x, u_y, 1)$. The matrix $\overline{\mathbf{B}}$ is always invertible and its eigenvalues are $1 + \zeta_x^2 + \zeta_y^2$ and 1 (of multiplicity two).

The Hamiltonian formulation of the reduced bracket in the physical variables (x, y, t, u_x, u_y, E) is non-canonical. The constrained Hamiltonian $\overline{\mathcal{H}}_c$ is obtained from the free-particle Hamiltonian $\overline{\mathcal{H}}$ in Eq. (6.2) replacing z by ζ and u_z by $u_x\zeta_x + u_y\zeta_y + \zeta_t$:

$$\overline{\mathcal{H}}_c = \frac{u_x^2 + u_y^2 + (\zeta_x u_x + \zeta_y u_y + \zeta_t)^2}{2} + \mathrm{g}\zeta + E. \tag{6.8}$$

Then, the equations of motion are given by

$$\frac{\mathrm{d}\overline{F}}{\mathrm{d}\tau} = \{\overline{F}, \overline{\mathcal{H}}_c\}_*, \tag{6.9}$$

where $\overline{F}$ is any of the dynamical variables and the non-canonical Poisson bracket is that in Eq. (6.3). It follows that

$$\frac{\mathrm{d}t}{\mathrm{d}\tau} = \{t, \overline{\mathcal{H}}_c\}_* = 1,$$

i.e., $t = \tau$ with a proper choice of the initial time. Then, the JS equations (5.8) are given by

$$\dot{x} = \frac{\mathrm{d}x}{\mathrm{d}t} = \{x, \overline{\mathcal{H}}_c\}_*, \qquad \dot{y} = \frac{\mathrm{d}y}{\mathrm{d}t} = \{y, \overline{\mathcal{H}}_c\}_*.$$

Furthermore, we get an equation for the evolution of the energy E as

$$\frac{\dot{E}}{\zeta_t} = \frac{\dot{u}_x}{\zeta_x} = \frac{\dot{u}_y}{\zeta_y}.$$

For a time-independent surface, the Poisson bracket obtained from Eq. (6.6) simplifies, since the variables (t, E) can be dropped. In this case, the Poisson matrix reduces to a 4×4 matrix

$$\mathbb{J}_1 = \begin{pmatrix} 0 & \mathbf{B}^{-1} \\ -(\mathbf{B}^{-1})^\dagger & \mathcal{B} \end{pmatrix},$$

where $\mathbf{B}$ is given by Eq. (5.9) and

$$\mathcal{B} = b_3 \begin{pmatrix} 0 & -1 \\ 1 & 0 \end{pmatrix}.$$

6.3. *Canonical Hamiltonian via Darboux theorem*

Following Darboux's theorem, using a change of variables it is possible to make the Poisson bracket obtained from Eq. (6.6), canonical. The choice of working either in canonical coordinates or non-canonical ones depends on the problem at hand, however they are equivalent (since it is an invertible change of coordinates). For instance, working with physical variables has the advantage of lending itself to a better intuition. Working with a canonical brackets might have some advantages, e.g., allowing the use of symplectic algorithms developed for canonical Hamiltonian systems.

Here we apply Darboux's algorithm by modifying the momenta u_x, u_y and E. In order to find the new momenta p_x, p_y and $\tilde{E}$ which are canonically conjugate to x, y and t respectively, one has to solve first order linear partial differential equations of the kind $\{x, p_x\} = 1$, e.g., using the method of characteristics. We restrict the search of these new variables to $p_x = p_x(x, y, t, u_x, u_y)$, $p_y = p_y(x, y, t, u_x, u_y)$ and $\tilde{E} = E + \varepsilon(x, y, t, u_x, u_y)$. After some algebra, the change of variables reads

$$\begin{aligned} p_x &= (1 + \zeta_x^2)u_x + \zeta_x\zeta_y u_y + \zeta_x\zeta_t, \\ p_y &= \zeta_x\zeta_y u_x + (1 + \zeta_y^2)u_y + \zeta_y\zeta_t, \\ \tilde{E} &= E + \zeta_t(u_x\zeta_x + u_y\zeta_y + \zeta_t). \end{aligned} \tag{6.10}$$

The first two equations yield the generalized momentum $\mathbf{p} = (p_x, p_y)$ as a function of the horizontal particle velocity $\mathbf{u}_h = (u_x, u_y)$ as in Eq. (5.10), i.e. $\mathbf{p} = \mathbf{B}\mathbf{u}_h + \boldsymbol{\alpha}$, where $\boldsymbol{\alpha}$ and $\mathbf{B}$ are given by Eq. (5.9). The Hamiltonian (6.8) in terms of the canonically conjugate variables $(\mathbf{x}, t)$ and $(\mathbf{p}, \tilde{E})$ becomes

$$\overline{\mathcal{H}}_c = \frac{1}{2}(\mathbf{p} - \boldsymbol{\alpha}) \cdot \mathbf{B}^{-1}(\mathbf{p} - \boldsymbol{\alpha}) + \mathrm{g}\zeta - \frac{\zeta_t^2}{2} + \tilde{E}.$$

This coincides with the Hamiltonian in Eq. (5.13) derived from the Lagrangian formalism, except for the extra variable $\tilde{E}$, canonically conjugate of the time t. The former is needed to make the system autonomous, as $\tilde{E}$ is the energy that the particle exchanges with the moving surface.

In the time-independent case ($\zeta_t = 0$), the additional variables (t, E) can be eliminated since the set of observables $F(x, y, p_x, p_y)$ constitutes a Poisson sub-algebra. The resulting Hamiltonian then reads

$$\mathcal{H}_c = \frac{1}{2}\mathbf{p} \cdot \mathbf{B}^{-1}\mathbf{p} + \mathrm{g}\zeta,$$

and $\mathbf{p} = \mathbf{B}\mathbf{u}_h$. This Hamiltonian resembles the one of the free particle, except that the metric for the kinetic energy is defined by $\mathbf{B}^{-1}$.

Another case of interest is the traveling wave $\zeta(x,y,t) = \overline{\zeta}(x-ct,y)$. Changing the dynamics to the moving frame with velocity c is a time-dependent change of coordinates, so it has to be performed in the autonomous framework. We perform a canonical transformation defined by $\overline{x} = x - ct$ and $\overline{E} = E + cp_x$, the other variables remain unchanged. Being canonical, this change of variables does not modify the expression of the bracket. The reduced (time-independent) Hamiltonian becomes

$$\mathcal{H}_c = \frac{1}{2}(\mathbf{p}-\boldsymbol{\alpha})\cdot\mathbf{B}^{-1}(\mathbf{p}-\boldsymbol{\alpha}) + \mathrm{g}\overline{\zeta} - c^2\frac{\overline{\zeta}_x^2}{2} - cp_x, \tag{6.11}$$

with $\boldsymbol{\alpha} = -c\overline{\zeta}_x(\overline{\zeta}_x, \overline{\zeta}_y)$, and the canonically conjugate variables are $(\overline{x}, p_x)$ and (y, p_y). Here, the matrix $\mathbf{B}$ is given by Eq. (5.9) where ζ is replaced by $\overline{\zeta}$.

Hamiltonian (6.11) can be written in the form

$$\mathcal{H}_c = \frac{1}{2}(\mathbf{p}-\boldsymbol{\alpha}-c\mathbf{B}\mathbf{e}_1)\cdot\mathbf{B}^{-1}(\mathbf{p}-\boldsymbol{\alpha}-c\mathbf{B}\mathbf{e}_1) + \mathrm{g}\overline{\zeta} - \frac{1}{2}c^2, \tag{6.12}$$

with $\mathbf{e}_1 = (1,0)^T$. Next, we express the Hamiltonian in terms of the particle velocity in the co-moving frame, $\overline{\mathbf{u}}_h = (\dot{\overline{x}}, \dot{y})$. From the fact that $\dot{\overline{x}} = \partial\mathcal{H}_c/\partial p_x$ and $\dot{y} = \partial\mathcal{H}_c/\partial p_y$, we have

$$\overline{\mathbf{u}}_h = \mathbf{B}^{-1}\left(\mathbf{p}-\boldsymbol{\alpha}-c\mathbf{B}\mathbf{e}_1\right).$$

Substitution in Eq. (6.12) yields,

$$\mathcal{H}_c = \frac{1}{2}\overline{\mathbf{u}}_h\cdot\mathbf{B}\overline{\mathbf{u}}_h + \mathrm{g}\overline{\zeta} - \frac{1}{2}c^2. \tag{6.13}$$

This form of the Hamiltonian will prove helpful in our analysis of the finite time blowup of the JS equations.

Finally, we concerning the one-dimensional case, e.g., when $\zeta_y = 0$. In this special case, the Hamiltonian simplifies to

$$\mathcal{H}_c = \frac{(p_x - \zeta_t\zeta_x)^2}{2(1+\zeta_x^2)} + \frac{{p_y}^2}{2} + \mathrm{g}\zeta - \frac{\zeta_t^2}{2}.$$

Since the potential does not depend on y, the momentum p_y is constant, so the motion in the y-direction is trivial. In the non-trivial direction, the reduced one-dimensional Hamiltonian becomes

$$\mathcal{H}_{1D} = \frac{(p_x - \zeta_t\zeta_x)^2}{2(1+\zeta_x^2)} + \mathrm{g}\zeta - \frac{\zeta_t^2}{2}.$$

6.4. *Physical interpretation of the vector* $\mathbf{b}_\mathrm{m}$ *in Eq.* (6.7)

The Poisson structure of particle motion on an unsteady surface bears some similarities with the motion of a charged particle in electromagnetic fields. In terms of the physical variables (position $\mathbf{x}$ and velocity $\mathbf{u}$), the Poisson bracket of a charge particle in a magnetic field is non-canonical with a part of the form $\mathbf{b}_\mathrm{m}\cdot(\partial_\mathbf{u}F\times\partial_\mathbf{u}G)$, called gyrobracket (responsible for the gyration motion of the particle around magnetic field lines) where $\mathbf{b}_\mathrm{m}$ is the magnetic field. In canonical coordinates, the velocity $\mathbf{u}$ has to be shifted by the vector potential $\mathbf{A}_\mathrm{m}$, which satisfies $\mathbf{b}_\mathrm{m} = \overline{\nabla}\times\mathbf{A}_\mathrm{m}$ (see Littlejohn (1979) for more details).

Our vector $\mathbf{b}_\mathrm{m}$ in Eq. (6.7) can be interpreted as a magnetic field in the extended phase space and the associated vector potential follows from

$$(1+|\nabla\zeta|^2)\mathbf{b}_\mathrm{m} = \overline{\nabla}\times\mathbf{A}_\mathrm{m},$$

with

$$\mathbf{A}_{\mathrm{m}} = -(u_x\zeta_x + u_y\zeta_y + \zeta_t)\overline{\nabla}\zeta.$$

Notice that in general $\mathbf{b}_{\mathrm{m}}$ is not divergence-free because of the factor $(1+|\nabla\zeta|^2)$. Furthermore, in Eq. (6.6), the term $\mathcal{B}$ generates a term $\mathbf{b}_{\mathrm{m}} \cdot \partial_{\mathbf{u}}F \times \partial_{\mathbf{u}}G$ in the Poisson bracket, since we notice that $\overline{\mathcal{B}}$ can be written as $\overline{\mathcal{B}} = \mathbf{b}_{\mathrm{m}}\times$, i.e. it maps a vector $\mathbf{v}$ into $\mathbf{b}_{\mathrm{m}} \times \mathbf{v}$. Whereas when the Poisson bracket is canonical, the momenta have to be shifted by the "vector potential" $\boldsymbol{\alpha}$ [see Eq. (5.10)].

Furthermore, the b_3 component of $\mathbf{b}_{\mathrm{m}}$ can be written as

$$b_3 = \frac{\nabla\zeta \times \nabla(u_x\zeta_x + u_y\zeta_y + \zeta_t)}{1 + |\nabla\zeta|^2}, \tag{6.14}$$

where we have used the two-dimensional cross-product. Comparing (6.14) to (3.16), we observe that $b_3 = \omega_3/2$ is half the vertical z component of the vorticity created on the free-surface $z = \zeta(x, y, t)$. Note that b_3 vanishes when the kinematic criterion (4.7) for wave breaking holds. We will not dwell too much on the geometric meaning of the components b_1 and b_2. We only point out that one can show that b_1 (b_2) is the z-component of space-time vorticity created on the space-time surface $z = \zeta(x, y, t)$. Thus, if we imagine trajectories $\overline{\mathbf{z}}(\tau)$ as those of "phase-space parcels" transported by the Hamiltonian flow velocity $\mathrm{d}\overline{\mathbf{z}}/\mathrm{d}\tau$, then the vector $\mathbf{b}_{\mathrm{m}}$ can be interpreted as space-time vorticity generated by the Hamiltonian flow. These observations will be useful below to interpret the symplectic forms associated with the Hamiltonian equations.

7. Symplectic structure

In terms of the canonically conjugate variables $(\mathbf{x}, t, \mathbf{p}, \tilde{E})$ the associated symplectic one-form is given by

$$\omega^1 = p_x\mathrm{d}x + p_y\mathrm{d}y + \tilde{E}\mathrm{d}t.$$

The two-form $\omega^2 = \mathrm{d}\omega^1$, which provides the symplectic structure of the dynamics, follows by exterior differentiation as

$$\omega^2 = \mathrm{d}p_x \wedge \mathrm{d}x + \mathrm{d}p_y \wedge \mathrm{d}y + \mathrm{d}\tilde{E} \wedge \mathrm{d}t.$$

To gain physical insights into the inviscid kinematics of fluid particles near large crests, it is convenient to write the above symplectic forms in terms of the non-canonical variables $\overline{\mathbf{z}} = (x, y, u_x, u_y, t, E)$. Using the transformations (6.10), we obtain

$$\begin{aligned}\omega^1 = \left((1+\zeta_x^2)u_x + \zeta_x\zeta_y u_y + \zeta_x\zeta_t\right)\mathrm{d}x + \left(\zeta_x\zeta_y u_x + (1+\zeta_y^2)u_y + \zeta_y\zeta_t\right)\mathrm{d}y \\ + \left(E + \zeta_t(\zeta_x u_x + \zeta_y u_y + \zeta_t)\right)\mathrm{d}t.\end{aligned} \tag{7.1}$$

To gain some intuition on the meaning of the above differential forms, we interpret the high-dimensional vector $\overline{\mathbf{z}} = (z_\alpha)$ as the trajectory of a 'fluid parcel' that is transported through the extended phase space by the Hamiltonian flow velocity

$$\mathrm{v}_H(\tau) = \frac{\mathrm{d}\overline{\mathbf{z}}}{\mathrm{d}\tau} = \left(\frac{\mathrm{d}z_\alpha}{\mathrm{d}\tau}\right),$$

where z_α is any of the non-canonical variables (x, y, u_x, u_y, t, E) and the associated velocity

$$\frac{\mathrm{d}z_\alpha}{\mathrm{d}\tau} = \{z_\alpha, \overline{\mathcal{H}}_c\}_*,$$

follows from the non-canonical Dirac bracket (6.3) (see also Eq. (6.9)). Then, the symplectic one-form (7.1) associated with the Hamiltonian flow can be interpreted as the

circulation of the velocity v_H along the infinitesimal path $\mathrm{d}\overline{\mathbf{z}}$. The associated two-form follows as (see also Appendix B):

$$\omega^2 = \overline{L}_*^{\alpha\beta}\mathrm{d}z_\alpha \wedge \mathrm{d}z_\beta/2,$$

where the Lagrange matrix $\overline{L}_*^{\alpha\beta}$ is the inverse of the Dirac-Poisson matrix (6.6), that is

$$\overline{\mathbb{L}}_* = \begin{pmatrix} (1+|\nabla\zeta|^2)\overline{\mathcal{B}} & -\overline{\mathbf{B}}^T \\ \overline{\mathbf{B}} & 0 \end{pmatrix}.$$

Furthermore,

$$\begin{aligned}\omega^2 = &-(1+|\nabla\zeta|^2)b_3\mathrm{d}x\wedge\mathrm{d}y + \mathrm{d}E\wedge\mathrm{d}t + (1+\zeta_x^2)\mathrm{d}u_x\wedge\mathrm{d}x \\ &+\zeta_x\zeta_y\mathrm{d}u_y\wedge\mathrm{d}x + \zeta_x\zeta_y\mathrm{d}u_x\wedge\mathrm{d}y + (1+\zeta_y^2)\mathrm{d}u_y\wedge\mathrm{d}y.\end{aligned} \tag{7.2}$$

On the slice $t=$ const of the extended phase space, the non-canonical one-form (7.1) simplifies to

$$\omega^1 = (\mathbf{B}\mathbf{u}_h + \boldsymbol{\alpha})\cdot\mathrm{d}\mathbf{x},$$

where we have used the identity in Eq. (5.10) and $\mathbf{u}_h = (u_x, u_y)$ is the horizontal particle velocity. The one-form ω^1 is invariant along closed material lines. This implies that if $\gamma(t)$ is a closed material line, the quantity

$$\mathcal{C}(t) = \oint_{\gamma(t)} (\mathbf{B}\mathbf{u}_h + \boldsymbol{\alpha})\cdot\mathrm{d}\mathbf{x},$$

is constant, i.e., it does not vary in time. Clearly, $\mathcal{C}(t)$ is the physical circulation induced by the particle motion given in Eq. (3.22), and is conserved by Kelvin's theorem (see, e.g. Eyink (2007)).

Furthermore, on $t=$ const. slices, the non-canonical two-form (7.2) reduces to

$$\begin{aligned}\omega^2 = &-(1+|\nabla\zeta|^2)b_3\mathrm{d}x\wedge\mathrm{d}y + (1+\zeta_x^2)\mathrm{d}u_x\wedge\mathrm{d}x \\ &+\zeta_x\zeta_y\mathrm{d}u_y\wedge\mathrm{d}x + \zeta_x\zeta_y\mathrm{d}u_x\wedge\mathrm{d}y + (1+\zeta_y^2)\mathrm{d}u_y\wedge\mathrm{d}y.\end{aligned} \tag{7.3}$$

Note that the coefficient b_3 of $\mathrm{d}x\wedge\mathrm{d}y$ is half the vertical component of the physical vorticity created on the free surface $z=\zeta(x,y,t)$ [see Eqs. (6.14) and (3.16)].

In Section 4 we have shown that vorticity vanishes at a surface crest, where $\zeta_x=\zeta_y=0$, when the horizontal particle velocity $\mathbf{u}_h$ equals the propagation speed $\mathbf{V}_c$ of the crest [see Eq. (4.7)], or equivalently when the kinematic criterion (4.6) for wave breaking holds. In this case the two-form (7.3) further simplifies to

$$\omega^2 = \mathrm{d}u_x\wedge\mathrm{d}x + \mathrm{d}u_y\wedge\mathrm{d}y. \tag{7.4}$$

and the associated Hamiltonian (6.8) reduces to

$$\overline{\mathcal{H}}_c = \frac{u_x^2+u_y^2+\zeta_t^2}{2} + \mathrm{g}\zeta + E. \tag{7.5}$$

This implies that if the kinematic criterion (4.6) is attained at the largest crest, i.e. when $\zeta_t=0$, then the two-form (7.4) and the associated Hamiltonian $\overline{\mathcal{H}}_c$ in (7.5) are those of a particle in free-flight, as if the surface on which the motion is constrained is non-existent and, as a result, vorticity is not created. Clearly, in realistic oceanic waves the large crest eventually breaks and energy of fluid particles is dissipated to turbulence as a clear manifestation of time irreversibility. This appears analogous to a flight–crash event in fluid turbulence, where a particle flies with a large velocity before suddenly losing energy (Xu *et al.* 2014). Clearly, the Hamiltonian dynamics is time-reversible and it may

reveals the inviscid mechanism of breaking inception before turbulent dissipative effects take place. To do so, the fluid particle kinematics on the free-surface must be coupled with the dynamics of the irrotational wave field that generates the surface exploiting Zakharov's (1968) Hamiltonian formalism.

8. There are no finite-time blowups

In the appendix of Sclavounos (2005), contributed by Bridges, the possibility of finite-time blowup of solutions of the JS equations is discussed. Bridges studies the special case of the particle kinematics on a 1D surface, i.e. when $\zeta_y \equiv 0$. The equations of motion in Eqs. (5.8) then reduce to

$$\dot{x} = u_x, \quad \dot{y} = u_y,$$

$$\dot{u}_x = -\frac{2\zeta_x\zeta_{xt}}{1+\zeta_x^2}u_x - \frac{\zeta_x\zeta_{xx}}{1+\zeta_x^2}u_x^2 - \frac{\zeta_x(\zeta_{tt}+\mathrm{g})}{1+\zeta_x^2}, \quad \dot{u}_y = 0.$$

It is then argued that under the further simplifying assumption that the matrix

$$\frac{\zeta_x}{1+\zeta_x^2}\begin{pmatrix}\zeta_{xx} & \zeta_{xt}\\ \zeta_{xt} & \zeta_{tt}+\mathrm{g}\end{pmatrix}$$

is constant along trajectories $x(t)$, the horizontal velocity u_1 is likely to grow unbounded in finite time. This latter assumption in particular implies that the first element of the above matrix is constant. Denoting this constant by K_0, we have

$$\frac{\zeta_x\zeta_{xx}}{1+\zeta_x^2}\Big|_{(x(t),t)} = \frac{1}{2}\frac{\partial}{\partial x}\ln\left(1+\zeta_x^2\right)\Big|_{(x(t),t)} = K_0.$$

Similarly, the off-diagonal elements of the matrix being constant along trajectories implies

$$\frac{\zeta_x\zeta_{xt}}{1+\zeta_x^2}\Big|_{(x(t),t)} = \frac{1}{2}\frac{\partial}{\partial t}\ln\left(1+\zeta_x^2\right)\Big|_{(x(t),t)} = K_1,$$

for some constant K_1.

Therefore Bridges' simplifying assumptions are highly specific and unrealistic. Nevertheless, his observation raises the fundamental question of whether the JS equations are well-posed. In fact, the right-hand-side of the JS equations (cf. Eq. (5.8)) is not Lipschitz continuous due to the presence of the quadratic terms in $\dot{x}$ and $\dot{y}$. Therefore, the elementary results from ODE theory (i.e., Picard's existence and uniqueness theorem) do not rule out the finite-time blowup scenario.

Our Hamiltonian formulation for the 3-D particle kinematics shows that for smooth steady surfaces (i.e. when $\zeta = \zeta(x,y)$ has bounded partial derivatives), the finite-time blowup never occurs. As we show in Appendix C, the mere conservation of a Hamiltonian function does not generally rule out the finite-time blowup. However, the particular form of the Hamiltonian function (5.14) leads to a finite bound on particle speed.

To see this, note that the Hamiltonian $\mathcal{H}_c = \mathcal{H}_c(\mathbf{x},\mathbf{p})$ derived in Eq. (5.14) is conserved along the trajectories $(\mathbf{x}(t),\mathbf{p}(t))$. More precisely,

$$\mathcal{H}_c(\mathbf{x}(t),\mathbf{p}(t)) = \mathcal{H}_c(\mathbf{x}(0),\mathbf{p}(0)) = \mathcal{H}_0 < \infty, \tag{8.2}$$

for all t and finite initial data $(\mathbf{x}(0),\mathbf{p}(0))$.

On the other hand,

$$\mathcal{H}_c(\mathbf{x},\mathbf{p}) = \frac{1}{2}\mathbf{p}\cdot\mathbf{B}^{-1}\mathbf{p} + \mathrm{g}\zeta(\mathbf{x}) \geqslant \frac{|\mathbf{p}|^2}{2(1+|\nabla\zeta(\mathbf{x})|^2)} + \mathrm{g}\zeta(\mathbf{x}), \tag{8.3}$$

where the inequality follows from the fact that $\mathbf{B}^{-1}$ is symmetric, positive-definite with the smallest eigenvalue equal to $(1+|\nabla\zeta|^2)^{-1}$.

Now assume that there exists a finite time t_0 such that $\lim_{t\to t_0}|\mathbf{p}(t)|=\infty$, i.e., there is a blowup at time t_0. Since ζ and $|\nabla\zeta|$ are bounded, inequality (8.3) implies that $\lim_{t\to t_0}\mathcal{H}_c(\mathbf{x}(t),\mathbf{p}(t))=\infty$. This, however, contradicts the conservation law (8.2).

By definition of the canonical momentum (5.10), we have $\mathbf{p}=\mathbf{B}\mathbf{u}_h$. This in turn implies

$$|\mathbf{p}|^2=\mathbf{u}_h\cdot\mathbf{B}^2\mathbf{u}_h\geqslant|\mathbf{u}_h|^2,$$

where the inequality follows from the fact that $\mathbf{B}$ is positive definite with the smallest eigenvalue equal to 1. Since $|\mathbf{p}|$ is bounded, so is $|\mathbf{u}_h|$, ruling out the finite-time blowup for the particle velocity. In summary, in the autonomous case (where the smooth surface ζ is time-independent) the equations of motion (5.8) are well-posed and finite-time blowup cannot occur.

For traveling waves, i.e., $\zeta(x,y,t)=\overline{\zeta}(x-ct,y)$, one can also show that there are no finite-time blowups. The proof is similar to the steady case, except that for the traveling waves the conserved Hamiltonian is given by Eq. (6.13). Namely, in the co-moving frame $\overline{\mathbf{x}}=(x-ct,y)$, we have

$$\mathcal{H}_c(\overline{\mathbf{x}}(t),\mathbf{p}(t))\geqslant\frac{|\mathbf{p}-\boldsymbol{\alpha}-c\mathbf{B}\mathbf{e}_1|^2}{2(1+|\nabla\zeta(\overline{\mathbf{x}})|^2)}+\mathrm{g}\overline{\zeta}(\overline{\mathbf{x}})-\frac{1}{2}c^2.$$

As in the steady case, blowup of $\mathbf{p}$ violates the conservation of the Hamiltonian function.

For the general non-autonomous case, where ζ is time-dependent, the finite-time blowup may not be ruled out by the above argument. We point out that in our numerical simulations of the JS equations with unsteady surfaces, we did not observe any trace of such singular behavior (Farazmand *et al.* 2015).

9. Trapping regions for steady flows and traveling waves

As mentioned earlier, the JS equations are very general as they describe the friction-less motion of a particle on a given surface. Using the Hamiltonian structure in Eq. (5.14), we show that the horizontal motion of a particle on a steady surface (i.e., $\zeta=\zeta(x,y)$) or on a traveling wave (i.e., $\zeta=\overline{\zeta}(x-ct,y)$) is always trapped in a subset of the two-dimensional $x-y$ plane. Since the Hamiltonian is conserved, the phase space $(x,y,u_x,u_y)\in\mathbb{R}^4$ is foliated by the invariant hypersurfaces $\mathcal{H}=$ const. These hypersurfaces are three-dimensional, and therefore, the particle trajectories can be chaotic. It turns out that one can deduce more from the Hamiltonian structure. Namely, we show that, based on their initial conditions, the trajectories are confined to a subset of the configuration space (x,y).

We first consider the steady case $\zeta_t=0$, where the Hamiltonian (6.8) can be written as

$$\mathcal{H}(\mathbf{x},\mathbf{u})=\mathrm{g}\zeta(\mathbf{x})+\frac{1}{2}|\mathbf{u}|^2+\frac{1}{2}|\mathbf{u}\cdot\nabla\zeta(\mathbf{x})|^2. \tag{9.1}$$

Note that the energy E is omitted since the system is autonomous. In this steady case, the following result holds.

Theorem 1. *Consider the motion of a particle constrained to the smooth steady surface $\zeta=\zeta(\mathbf{x})$. Denote the initial condition of the particle by $(\mathbf{x}_0,\mathbf{u}_0)$ and define*

$$D_0:=\left\{\mathbf{x}=(x,y)\in\mathbb{R}^2|\zeta(\mathbf{x})\leqslant\zeta(\mathbf{x}_0)+\frac{1}{2g}|\mathbf{u}_0|^2+\frac{1}{2g}|\mathbf{u}_0\cdot\nabla\zeta(\mathbf{x}_0)|^2\right\}. \tag{9.2}$$

The position of the particle is bound to the subset D_0, i.e. $(x(t), y(t)) \in D_0$ for all times t.

Proof. Hamiltonian (9.1) is conserved along particle trajectories $(\mathbf{x}(t), \mathbf{u}(t))$. Hence we have

$$\mathrm{g}\zeta(\mathbf{x}(t)) \leqslant \mathcal{H}(\mathbf{x}(t), \mathbf{u}(t)) = \mathcal{H}(\mathbf{x}_0, \mathbf{u}_0).$$

□

Note that the above theorem does not imply that the subset D_0 is invariant. In fact, particles initiated outside D_0 can very well enter (and exit) the set. Instead, the set D_0 is a *trapping region*, i.e., particles starting in D_0 with initial conditions $(\mathbf{x}_0, \mathbf{u}_0)$ stay in D_0 for all times. For a given surface, the trapping region D_0 is entirely determined by the initial position $\mathbf{x}_0$ and the initial velocity $\mathbf{u}_0$ of the particle.

An interesting special case is to consider the motion of the particle from rest, i.e., zero initial velocity. Then Theorem 1 implies the following.

Corollary 1. *Consider the motion of a particle that is initially at rest and moves on a smooth steady surface $\zeta = \zeta(x, y)$. Denote the initial position of the particle by (x_0, y_0) and define*

$$D_0 := \left\{(x, y) \in \mathbb{R}^2 | \zeta(x, y) \leqslant \zeta(x_0, y_0)\right\}.$$

The position of the particle is bound to the subset D_0, i.e. $(x(t), y(t)) \in D_0$ for all times t.

Proof. This is a direct consequence of Theorem 1 with the initial velocity $\mathbf{u}_0 = \mathbf{0}$. □

Theorem 1 and Corollary 1 hold for traveling waves, $\zeta(x, y, t) = \overline{\zeta}(x - ct, y)$. The statements are identical except that the coordinate x and the velocity u_x are replaced with the co-moving coordinate $\bar{x} = x - ct$ and velocity $\bar{u}_x = \dot{x} - c$, respectively. The proofs are similar and therefore omitted here. The trapping region in Eq. (9.2) is now given by

$$D_0 := \left\{\mathbf{x} = (\bar{x}, y) \in \mathbb{R}^2 | \overline{\zeta}(\mathbf{x}) \leqslant \overline{\zeta}(\mathbf{x}_0) + \frac{1}{2\mathrm{g}}|\mathbf{u}_0 - c\mathbf{e}_1|^2 + \frac{1}{2\mathrm{g}}|(\mathbf{u}_0 - c\mathbf{e}_1) \cdot \nabla\overline{\zeta}(\mathbf{x}_0)|^2\right\},$$

where $\mathbf{e}_1$ is the unit vector along $\bar{x}$ and the initial particle velocity $\mathbf{u}_0$ is that in the fixed reference frame.

10. Concluding remarks

We have investigated the properties of the JS equations for the kinematics of fluid particles on the sea surface. We showed that the JS equations can be derived from a Lagrangian principle describing the motion of a frictionless particle constrained on an unsteady surface and subject to gravity. Further, for a zero-stress free surface the classical kinematic criterion for wave breaking is deduced from the condition of vanishing of vorticity generated at a crest. If this holds for the largest crest, the Hamiltonian structure of the JS equations reveals that the associated symplectic two-form instantaneously reduces to that of the motion of a particle in free flight, as if the constraint to be on the free surface did not exist. Finally, for steady surfaces and traveling waves particle velocities remain bounded at all times, ruling out the finite-time blowup of solutions.

11. Acknowledgments

FF acknowledges the Georgia Tech graduate courses 'Classical Mechanics II' taught by Jean Bellissard in Spring 2013 and 'Nonlinear dynamics: Chaos, and what to do about it?' taught by Predrag Cvitanović in Spring 2012. FF also thanks Jean Bellissard for stimulating discussions on differential geometry and classical mechanics as well as for a revision of an early draft of the manuscript. The authors are also grateful to Jean Bellissard, Predrag Cvitanović and Rafael De La Llave for stimulating discussions on symplectic geometry and Hamiltonian dynamics.

A. JS equations for steady irrotational flows

Consider a one-dimensional, semi-infinite, steady, irrotational flow constrained to the wave surface $\zeta = \zeta(x)$. These assumption imply $\phi_y = \phi_t = 0$ (where ϕ is the velocity potential) and $\zeta_y = \zeta_t = 0$. Since the vertical particle velocity satisfies

$$\dot{z} = \phi_z(x(t), z(t)),$$

the respective acceleration is given by

$$\ddot{z} = \phi_{xz}\dot{x} + \phi_{zz}\dot{z}.$$

For particles on the surface, $z(t) = \zeta(x(t))$, which implies

$$\dot{z} = \zeta_x \dot{x},$$

and

$$\ddot{z} = \zeta_{xx}\dot{x}^2 + \zeta_x \ddot{x}.$$

Therefore,

$$\zeta_{xx}\dot{x}^2 + \zeta_x\ddot{x} = \phi_{xz}\dot{x} + \phi_{zz}\zeta_x\dot{x},$$

which upon multiplying by ζ_x and rearranging terms gives

$$\zeta_x^2\ddot{x} = -\zeta_{xx}\zeta_x\dot{x}^2 + \phi_{xz}\zeta_x\dot{x} + \phi_{zz}\zeta_x^2\dot{x}. \tag{A.1}$$

On the other hand, the Bernoulli equation (4.9) reads

$$g\zeta(x(t)) + \frac{1}{2}(\dot{x}^2 + \phi_z^2(x(t), \zeta(x(t))) = 0.$$

Taking the derivative with respect to time we obtain

$$\ddot{x} = -g\zeta_x - \phi_z\big(\phi_{xz} + \phi_{zz}\zeta_x\big).$$

Using $\phi_z = \dot{z} = \zeta_x\dot{x}$ implies

$$\ddot{x} = -g\zeta_x - \phi_{xz}\zeta_x\dot{x} - \phi_{zz}\zeta_x^2\dot{x}. \tag{A.2}$$

Adding Eqs. (A.1) and (A.2) gives the JS equations (5.8) in the case of 1-D steady flows.

B. Symplectic forms

The forms ω^2 in Eq. (7.2) and ω^1 in Eq. (7.1) can be written more elegantly as

$$\omega^2 = \omega_{\mathrm{c}}^2 + \mathrm{d}(u_x\zeta_x + u_y\zeta_y + \zeta_t) \wedge \mathrm{d}\zeta,$$
$$\omega^1 = \omega_{\mathrm{c}}^1 + (u_x\zeta_x + u_y\zeta_y + \zeta_t)\mathrm{d}\zeta,$$

where

$$\omega_{\mathrm{c}}^2 = \mathrm{d}u_x \wedge \mathrm{d}x + \mathrm{d}u_y \wedge \mathrm{d}y + \mathrm{d}E \wedge \mathrm{d}t$$

is the two-form associated with the horizontal motion of a free-particle and

$$\omega_{\mathrm{c}}^1 = u_x \mathrm{d}x + u_y \mathrm{d}y + E\mathrm{d}t$$

the corresponding one-form. If we define $(z, u_z) = \varphi(x, y, t, u_x, u_y) = (\zeta, u_x\zeta_x + u_y\zeta_y + \zeta_t)$ as suggested by the two constraints in Eq. (6.5), the one- and two-forms associated with the constrained particle motion can be written using the pullback φ^*

$$\omega^2 = \omega_{\mathrm{c}}^2 + \varphi^*(\mathrm{d}u_z \wedge \mathrm{d}z),$$
$$\omega^1 = \omega_{\mathrm{c}}^1 + \varphi^*(u_z \mathrm{d}z).$$

C. The Hamiltonian structure of a prototype blowup problem

As a toy problem, Bridges considers the simplest second order ODE Riccatti equation, which can be written as

$$\dot{x} = u, \qquad \dot{u} = u^2. \tag{C.1}$$

Although the JS equations cannot be reduced to this form, we discuss its properties for completeness. The system (C.1) possesses the Hamiltonian

$$H = u\mathrm{e}^{-x},$$

which is of course an invariant of the dynamics. The non-canonical Poisson bracket is given by

$$\{F, G\} = u\mathrm{e}^x \left(\frac{\partial F}{\partial x}\frac{\partial G}{\partial u} - \frac{\partial F}{\partial u}\frac{\partial G}{\partial x} \right).$$

The canonical structure of the system is obtained in the variables $(x, \mathrm{e}^x \ln u)$.

For initial conditions (x_0, u_0) at $t = 0$

$$x(t) = x_0 + \ln \frac{1}{1 - u_0 t}, \qquad u(t) = \frac{u_0}{1 - u_0 t}.$$

Clearly, for positive initial velocities ($u_0 > 0$), all solutions blow up in finite time, with the time of blowup inversely proportional to the norm of the initial velocity data. On the other hand, trajectories are bounded for negative initial velocities and they exist for all time.

The finite-time singularity of the system can be explained exploiting the time invariance of the Hamiltonian $H = u\mathrm{e}^{-x}$. As u linearly tends to infinity when t tends to some t_0, x also tends to infinity, but logarithmically, when t goes to t_0, in such a way that the product between u and e^{-x}. This is possible because e^{-x} is not bounded from below by a strictly positive quantity. Contrast this with Eq. (8.3), where the quadratic part of the Hamiltonian is positive definite, and hence bounded from below by a positive constant.

REFERENCES

Banner, M. L., Barthelemy, X., Fedele, F., Allis, M., Benetazzo, A., Dias, F. & Peirson, W. L. 2014 Linking reduced breaking crest speeds to unsteady nonlinear water wave group behavior. *Phys. Rev. Lett.* **112**, 114502.

Banner, M L & Peregrine, D H 1993 Wave breaking in deep water. *Annual Review of Fluid Mechanics* **25** (1), 373–397.

Barthelemy, X., Banner, M.L., Peirson, W.L., Dias, F., & Allis, M. 2015*a* On the local properties of highly nonlinear unsteady gravity water waves. part 1. slowdown, kinematics and energetics. *Journal of Fluid Mechanics (submitted) http://arxiv.org/abs/1508.06001* .

Barthelemy, X., Banner, M.L., Peirson, W.L., Fedele, F., Allis, M. & Dias,

F. 2015*b* On the local properties of highly nonlinear unsteady gravity water waves. part 2. dynamics and onset of breaking. *Journal of Fluid Mechanics (submitted) http://arxiv.org/abs/1508.06002* .

Bridges, Thomas J. 2004 Superharmonic instability, homoclinic torus bifurcation and water-wave breaking. *Journal of Fluid Mechanics* **505**, 153–162.

Bridges, Thomas J., Hydon, Peter E. & S., Reich 2005 Vorticity and symplecticity in lagrangian fluid dynamics. *Journal of Physics A: Mathematical and General* **38** (6), 1403.

Chandre, C. 2013 Casimir invariants and the jacobi identity in dirac's theory of constrained hamiltonian systems. *Journal of Physics A: Mathematical and General* **46** (375201).

Chandre, C., de Guillebon, L., Back, A., Tassi, E. & Morrison, P.J. 2013 On the use of projectors for hamiltonian systems and their relationship with dirac brackets. *Journal of Physics A: Mathematical and Theoretical* **46**, 125203.

Dirac, P.A.M. 1950 Generalized hamiltonian dynamics. *Canadian Journal of Mathematics* **2**, 129.

Dirac, P.A.M. 1958 Generalized hamiltonian dynamics. *Proceedings of the Royal Society of London A: Mathematical, Physical and Engineering Sciences* **246**, 326.

Duncan, J. H., Qiao, H., Philomin, V. & Wenz, A. 1999 Gentle spilling breakers: crest profile evolution. *Journal of Fluid Mechanics* **379**, 191–222.

Eyink, G. L. 2007 "turbulence theory" course notes. *Tech. Rep.*. The Johns Hopkins University.

Farazmand, M., Fedele, F. & Chandre, C. 2015 Fluid particle kinematics on the ocean surface. part 2: phase-space geometry. *Journal of Fluid Mechanics (in preparation)* .

Fedele, F. 2014 Geometric phases of water waves. *EPL (Europhysics Letters)* **107** (6), 69001.

John, Fritz 1953 Two-dimensional potential flows with a free boundary. *Communications on Pure and Applied Mathematics* **6** (4), 497–503.

Krasitskii, V. P. 1994 On reduced equations in the Hamiltonian theory of weakly nonlinear surface waves. *J. Fluid Mech* **272**, 1–20.

Kurnia, R. & van Groesen, E. 2014 High order hamiltonian water wave models with wave-breaking mechanism. *Coastal Engineering* **93**, 55 – 70.

Littlejohn, R.G. 1979 A guiding center hamiltonian: A new approach. *Journal of Mathematical Physics* **20**, 2445.

Longuet-Higgins, M.S. 1998 Vorticity and curvature at a free surface. *Journal of Fluid Mechanics* **356**, 149–153.

Longuet-Higgins, M. S. 1978 The instabilities of gravity waves of finite amplitude in deep water. i. superharmonics. *Proceedings of the Royal Society of London. A. Mathematical and Physical Sciences* **360** (1703), 471–488.

Longuet-Higgins, Michael S. 1992 Capillary rollers and bores. *Journal of Fluid Mechanics* **240**, 659–679.

Longuet-Higgins, M. S. & Cleaver, R. P. 1994 Crest instabilities of gravity waves. part 1. the almost-highest wave. *Journal of Fluid Mechanics* **258**, 115–129.

Longuet-Higgins, M. S. & Fox, M. J. H. 1977 Theory of the almost-highest wave: the inner solution. *J. Fluid Mech.* **80**, 721–741.

Longuet-Higgins, M. S. & Fox, M. J. H. 1978 Theory of the almost-highest wave. Part 2. Matching and analytic extension. *Journal of Fluid Mechanics* **85**, 769–786.

Lundgren, T. & Koumoutsakos, P. 1999 On the generation of vorticity at a free surface. *Journal of Fluid Mechanics* **382**, 351–366.

Morrison, P. J. 1998 Hamiltonian description of the ideal fluid. *Rev. Mod. Phys.* **70(2)**, 467–521.

Perlin, M., Choi, W. & Tian, Z. 2013 Breaking waves in deep and intermediate waters. *Annual Review of Fluid Mechanics* **45** (1), 115–145.

Qiao, H. & Duncan, J. H. 2001 Gentle spilling breakers: crest flow-field evolution. *Journal of Fluid Mechanics* **439**, 57–85.

Rapp, R. J. & Melville, W. K. 1990 Laboratory measurements of deep-water breaking waves. *Philosophical Transactions of the Royal Society of London. Series A, Mathematical and Physical Sciences* **331** (1622), 735–800.

Saket, A., Peirson, W.L., Banner, M.L., Barthelemy, X. & Allis, M. 2015 Wave breaking onset of two–dimensional deep–water wave groups in the presence and absence of wind. *http://arxiv.org/abs/1508.07702* .

Sclavounos, P. D. 2005 Nonlinear particle kinematics of ocean waves. *J. Fluid Mech.* **540**, 133–142.

Shemer, L. 2013 On kinematics of very steep waves. *Natural Hazards and Earth System Science* **13** (8), 2101–2107.

Shemer, L. & Ee, B. K. 2015 Steep unidirectional wave groups – fully nonlinear simulations vs. experiments. *Nonlinear Processes in Geophysics Discussions* **2** (4), 1159–1195.

Shemer, L. & Liberzon, D. 2014 Lagrangian kinematics of steep waves up to the inception of a spilling breaker. *Physics of Fluids* **26** (1), 016601.

Song, Jin-Bao & Banner, Michael L. 2002 On determining the onset and strength of breaking for deep water waves. part i: Unforced irrotational wave groups. *Journal of Physical Oceanography* **32** (9), 2541–2558.

Stansell, P. & MacFarlane, C. 2002 Experimental investigation of wave breaking criteria based on wave phase speeds. *Journal of Physical Oceanography* **32** (5), 1269–1283.

Tulin, M. P. 2007 On the transport of energy in water waves.

Wu, J.Z. 1995 A theory of three dimensional interfacial vorticity dynamics. *Physics of Fluids* **7** (10), 2375–2395.

Xu, H., Pumir, A., Falkovich, G., Bodenschatz, E., Shats, M., Xia, H., Francois, N. & Boffetta, G. 2014 Flight–crash events in turbulence. *Proceedings of the National Academy of Sciences* **111** (21), 7558–7563.

Zakharov, V. E. 1968 Stability of periodic waves of finite amplitude on the surface of a deep fluid. *J. Appl. Mech. Tech. Phys.* **9**, 190–194.

Zakharov, V. E. 1999 Statistical theory of gravity and capillary waves on the surface of a finite-depth fluid. *Eur. J. Mech. B/Fluids* **18** (3), 327–344.